How tightly does calcite e-twin constrain stress?

Atsushi Yamaji[a,*]

[a] *Division of Earth and Planetary Sciences, Graduate School of Science, Kyoto University, Kyoto 606-8502, Japan*

Abstract

Mechanical twinning along calcite e-planes has been used for paleostress analyses. Since the twinning has a critical resolved shear stress at ~10 MPa, not only principal stress axes but also differential stress can be determined from the twins. In this article, five-dimensional stress space used in plasticity theory was introduced to describe the yield loci of calcite e-twinning. The constraints to paleostress from twin and untwin data and from calcite grains twinned on 0, 1, 2 and 3 e-planes were quantified by using their information contents, which were defined in the stress space. The orientations of twinned and untwinned e-planes are known to constrain not only stress axes but also differential stress, D, but they loose the resolution of D if the twin lamellae were formed at D greater than 50–100 MPa. On the other hand, it is difficult to observe twin lamellae subparallel to a thin section. The sampling bias due to this difficulty may give rise to distortive effect to the constraints especially to the determination of D. The stochastic modeling of this effect showed that 20–25% of twin lamellae can be overlooked.

Keywords: , mechanical twin, yield locus, differential stress space, information content, sampling bias, paleostress

1. Introduction

Calcite e-twinning is useful for understanding tectonics in the upper crust, because calcite is a common mineral and records deformations at low temperatures and low differential stresses (e.g., Turner, 1953; Groshong, 1972; Jamison and Spang, 1976; Laurent et al., 1981; Pfiffner and Burkhard, 1987; Burkhard, 1993; Constantin et al., 2007; Lacombe, 2010). Calcite e-twin has been used to infer not only the orientations but also the magnitudes of paleostresses.

In this paper, the theoretical analyses of Takeshita et al. (1987), Fry (2001) and Sato and Yamaji (2006) are reformulated to relate stress and the orientations of twinned and untwinned e-planes to define the yield locus of calcite e-twinning and to quantify the constraints from e-twin lamellae. The present study is based on the fact that the twinning occurs if resolved shear stress along the gliding direction of a twin plane exceeds a critical value, τ_c, which is assumed to be 10 MPa (Lacombe, 2010, and references therein) throughout of this paper, meaning that the twins are useful to investigate tectonics at the depths of about 0.5 to 5 km (Lacombe, 2007; Lacombe et al., 2009).

Here, we introduce, first, the five-dimensional stress space in which the yield loci of e-twinning is defined. Second, by using information theory, the constraints from twin and untwin data are quantitatively estimated, because several researchers utilized not only the attitudes of twinned e-planes but also those of untwinned ones in their stress inversion (Laurent et al., 1981, 1990; Etchecopar, 1984). Fry (2001, Fig. 3) explained why untwin data are necessary to constrain differential stress. The constraints from grains twinned on 0, 1, 2 and 3 e-planes are evaluated as well. In case the number density of twin lamellae is low, attention must be payed to sampling bias. It is shown that 20–25% of twin lamellae are overlooked due to the low angles made by the lamellae and the observation plane, e.g., a thin section. Thus, the bias can have distortive effects on paleostress analysis.

2. Notations and basic equations

In this section we introduce mathematical symbols and important terms for the following analyses. Let $\boldsymbol{c}$ be the unit vector indicating the host c-axis of a twin lamella, the unit normal of which is denoted by $\boldsymbol{e}$ (Table 1). The vectors are represented by (3×1)-matrices. The angle made by $\boldsymbol{c}$ and $\boldsymbol{e}$ is denoted by α, which is about 26.25° (Twiss and Moores, 2006, p. 499). We pay attention to the 'footwall' of a twin lamella to consider the gliding direction and shear stress on the lamella. Corresponding to the choice that compression is positive in sign, the unit normal, $\boldsymbol{e}$, is defined to point inward of the footwall block (e.g., Yamaji, 2007, p. 62). The unit vector, $\boldsymbol{g}$, indicates the gliding direction of the footwall. This vector can be calculated from $\boldsymbol{c}$ and $\boldsymbol{e}$,

$$\boldsymbol{g} = \boldsymbol{P}(\boldsymbol{c} - \boldsymbol{e}) \,/\, |\boldsymbol{P}(\boldsymbol{c} - \boldsymbol{e})|\,, \tag{1}$$

where the (3×3)-matrix, $\boldsymbol{P} \equiv \boldsymbol{I} - \boldsymbol{e}\boldsymbol{e}^{\mathrm{T}}$, is called elementary orthogonal projector (Meyer, 2000, p. 322), by which $\boldsymbol{c} - \boldsymbol{e}$ is orthogonally projected onto the twin plane.

A calcite grain has three sets of planes for e-twinning, which have three-fold symmetry about the c-axis. A set of e-planes is characterized by the paired vectors, $\boldsymbol{e}$ and $\boldsymbol{g}$. Each of the three sets has two states, twinned or untwinned. Following Venkitasubramanyan (1971), we refer to calcite grains with 1, 2 and 3

*Phone: +81 75 753 4266; fax: +81 75 753 4189.
Email address: yamaji@kueps.kyoto-u.ac.jp (Atsushi Yamaji)

twinned planes as singlets, doublets and triplets, respectively. In addition, we use the term, 'zeroplets,' to refer to untwinned grains.

Twinning is assumed to occur on a twin set if the resolved shear stress parallel to the gliding direction, τ, satisfies

$$\tau \geq \tau_c. \tag{2}$$

Otherwise, the potential set is left untwinned. A stress tensor is said to be compatible with a twin datum, if this condition is met on the e-plane from which the datum is obtained. Likewise, a stress tensor is said to be compatible with an untwin datum, if this condition does not hold on an untwinned e-plane. A stress tensor is said to explain a twin datum, if Eq. (2) is satisfied on the e-plane.

Given a stress tensor, $\boldsymbol{\sigma}$, the vectorial shear stress and resolved shear stress are given by $\boldsymbol{s} = \boldsymbol{P}\boldsymbol{\sigma}\boldsymbol{e}$ and

$$\tau = -\boldsymbol{g}^{\mathrm{T}}\boldsymbol{s} = -|\boldsymbol{s}|\cos\theta, \tag{3}$$

respectively, where θ is the angle made by $\boldsymbol{s}$ and $\boldsymbol{g}$. The minus signs in Eq. (3) correspond to the fact that deformation occurs in the direction to relieve stress.

The lateral translation of Mohr circles on a Mohr diagram does not affect shear stresses. Accordingly, we assume that the minimum principal stress equals zero, and consider the stress tensor of the form,

$$\boldsymbol{\sigma} = \boldsymbol{\sigma}^0 D, \tag{4}$$

where $D = \sigma_1 - \sigma_3$ is differential stress, and

$$\boldsymbol{\sigma}^0 = \boldsymbol{Q}\,\mathrm{diag}(1, \Phi, 0)\,\boldsymbol{Q}^{\mathrm{T}}, \tag{5}$$

$\boldsymbol{Q}$ the orthogonal matrix representing the principal orientations, and $\Phi = (\sigma_2 - \sigma_3)/(\sigma_1 - \sigma_3)$. Φ is called stress ratio, and has a value between 0 and 1. It follows from Eqs. (3) and (4) that

$$\tau = -\boldsymbol{g}^{\mathrm{T}}\boldsymbol{\sigma}^0\boldsymbol{e}D. \tag{6}$$

The tensor, $\boldsymbol{\sigma}^0$, carries the information of the attitude ($\boldsymbol{Q}$) and shape (Φ) of stress ellipsoid, the size of which is denoted by D.

3. Yield locus

In this section, we introduce the yield locus of calcite e-twinning. The locus is represented by a solid figure in five-dimensional stress space. Although the space and the locus are the concepts of abstract plasticity theory, it is worth introducing them, because (1) not only a multi-axial state of stress but also twin and untwin data are represented by position vectors in the space, and (2) the constraints from twin and untwin data on differential stress have geometric interpretations. In addition, the constraints from twin and untwin data are quantitatively estimated in the space.

3.1. Sigma- and epsilon-vectors

It is convenient for theoretical considerations to introduce the deviatoric stress tensor,

$$\boldsymbol{T} = \boldsymbol{\sigma} - \left(\frac{\sigma_1 + \sigma_2 + \sigma_3}{3}\right)\boldsymbol{I}.$$

Combining Eqs. (4) and (5), we have $\sigma_3 = 0, \sigma_2 = \Phi D, \sigma_1 = D$ and

$$\boldsymbol{T} = \left(\boldsymbol{\sigma}^0 - \frac{\Phi + 1}{3}\boldsymbol{I}\right)D, \tag{7}$$

Now, suppose the tensor,

$$\boldsymbol{\varsigma} = \frac{1}{\lambda}\left(\boldsymbol{\sigma}^0 - \frac{\Phi + 1}{3}\boldsymbol{I}\right), \tag{8}$$

where the denominator in the right-hand side of this equation,

$$\lambda = \sqrt{\frac{\Phi^2 - \Phi + 1}{3}}, \tag{9}$$

is always positive in sign, and has the minimum, 1/2, at $\Phi = 1/2$ and the maxima, $1/\sqrt{3} \approx 0.58$, at $\Phi = 0$ and 1. Then, Eq. (7) is rewritten as $\boldsymbol{T} = \boldsymbol{\varsigma}\lambda D$. The tensor, $\boldsymbol{\varsigma}$, has the second basic invariant,

$$\varsigma_{\mathrm{II}} \equiv \frac{1}{2}(\boldsymbol{\varsigma} : \boldsymbol{\varsigma}) = \frac{1}{2}(\varsigma_{11}^2 + \varsigma_{22}^2 + \varsigma_{33}^2) + \varsigma_{23}^2 + \varsigma_{31}^2 + \varsigma_{12}^2 = 1, \tag{10}$$

where the colon denotes the inner product of square matrices, $\boldsymbol{A} = (A_{ij})$ and $\boldsymbol{B} = (B_{ij})$, such that

$$\boldsymbol{A} : \boldsymbol{B} = \sum_{i,j}^{3} A_{ij}B_{ij}.$$

The second basic invariant of $\boldsymbol{T}$ is $T_{\mathrm{II}} = (\lambda D)^2$. The scalar quantity, $\sigma_e = \sqrt{3T_{\mathrm{II}}} = \sqrt{3}\lambda D$, is known as equivalent stress, which is used to predict yielding under multiaxial loading conditions (e.g., Hill, 1998). σ_e coincides with differential stress for axial stresses ($\Phi = 0$ or 1). $\boldsymbol{\varsigma}$ is the reduced stress tensor normalized by the conditions, trace $\boldsymbol{\varsigma} = 0$ and $\varsigma_{\mathrm{II}} = 1$, and has the form (Sato and Yamaji, 2006),

$$\boldsymbol{\varsigma} = \boldsymbol{Q}\left[\frac{\mathrm{diag}\,(2 - \Phi, 2\Phi - 1, -\Phi - 1)}{3\lambda}\right]\boldsymbol{Q}^{\mathrm{T}}.$$

Resolved shear stress, τ, can be expressed in terms of $\boldsymbol{\varsigma}$. It follows from Eq. (8) that

$$\boldsymbol{\sigma}^0 = \lambda\boldsymbol{\varsigma} + \left(\frac{\Phi + 1}{3}\right)\boldsymbol{I}. \tag{11}$$

Substituting Eq. (11) into (6), we find that an equation similar to Eq. (6) holds for the tensor, $\boldsymbol{\varsigma}$,

$$\tau = -\boldsymbol{g}^{\mathrm{T}}\left(\lambda\boldsymbol{\varsigma} + \frac{\Phi + 1}{3}\boldsymbol{I}\right)\boldsymbol{e}D = -\lambda D\boldsymbol{g}^{\mathrm{T}}\boldsymbol{\varsigma}\boldsymbol{e}, \tag{12}$$

where the term, $\boldsymbol{g}^{\mathrm{T}}\boldsymbol{I}\boldsymbol{e}$, vanished due to the orthogonality of $\boldsymbol{e}$ and $\boldsymbol{g}$. These vectors are exchangeable in this equation, so we obtain

$$\tau = -\frac{1}{2}\left(\boldsymbol{g}^{\mathrm{T}}\boldsymbol{\varsigma}\boldsymbol{e} + \boldsymbol{e}^{\mathrm{T}}\boldsymbol{\varsigma}\boldsymbol{g}\right)\lambda D. \tag{13}$$

The constraints of twin and untwin data are represented by geometrical conditions in the five-dimensional space. Now, we derive strain tensor for a twin datum to introduce the conditions. Generally, infinitesimal strain tensor has the expression,

$$\boldsymbol{E} = \frac{1}{2}\left[\nabla\boldsymbol{u} + (\nabla\boldsymbol{u})^{\mathrm{T}}\right], \tag{14}$$

where $\boldsymbol{u}$ is displacement vector, and $\nabla\boldsymbol{u}$ is displacement gradient tensor. E-twinning results in simple shear along an e-plane. Let us use the coordinate system with the first and second coordinates parallel to $\boldsymbol{g}$ and $\boldsymbol{e}$, respectively. Then, the displacement associated with twinning is written as $\boldsymbol{u}' = (\gamma\xi, 0, 0)^{\mathrm{T}}$, where γ is shear strain, and ξ is the distance from the e-plane. Thus, we have

$$\nabla\boldsymbol{u}' = \begin{pmatrix} 0 & \gamma & 0 \\ 0 & 0 & 0 \\ 0 & 0 & 0 \end{pmatrix},$$

in the coordinate system. Let $\boldsymbol{b}$ be the unit vector perpendicular to $\boldsymbol{g}$ and $\boldsymbol{e}$, i.e., $\boldsymbol{b} = \boldsymbol{g} \times \boldsymbol{e}$. Then, the orthogonal matrix,

$$\boldsymbol{R} = \begin{pmatrix} g_1 & e_1 & b_1 \\ g_2 & e_2 & b_2 \\ g_3 & e_3 & b_3 \end{pmatrix},$$

transforms $\nabla\boldsymbol{u}'$ to $\nabla\boldsymbol{u}$, the components of which are described in a coordinate system that is taken independently from the e-plane in question. That is, we have

$$\nabla\boldsymbol{u} = \boldsymbol{R}\,(\nabla\boldsymbol{u}')\,\boldsymbol{R}^{\mathrm{T}} = \gamma\boldsymbol{g}\boldsymbol{e}^{\mathrm{T}} = \gamma\begin{pmatrix} g_1e_1 & g_1e_2 & g_1e_3 \\ g_2e_1 & g_2e_2 & g_2e_3 \\ g_3e_1 & g_3e_2 & g_3e_3 \end{pmatrix}. \tag{15}$$

It follows from Eqs. (14) and (15) that the simple shear by e-twinning has the strain tensor,

$$\boldsymbol{E} = \frac{\gamma}{2}\left(\boldsymbol{g}\boldsymbol{e}^{\mathrm{T}} + \boldsymbol{e}\boldsymbol{g}^{\mathrm{T}}\right).$$

The magnitude of this tensor is denoted by γ, and the content of the parentheses bears the information of the direction of strain: The role of γ in $\boldsymbol{E}$ is comparable with that of D in $\boldsymbol{\sigma}$. Just like the information of stress magnitude has been abstracted away from $\boldsymbol{\varsigma}$, we omit γ to define the reduced strain tensor,

$$\begin{aligned}\boldsymbol{\varepsilon} &= \boldsymbol{g}\boldsymbol{e}^{\mathrm{T}} + \boldsymbol{e}\boldsymbol{g}^{\mathrm{T}} \\ &= \begin{pmatrix} 2g_1e_1 & g_1e_2 + g_2e_1 & g_1e_3 + g_3e_1 \\ g_2e_1 + g_1e_2 & 2g_2e_2 & g_2e_3 + g_3e_2 \\ g_3e_1 + g_1e_3 & g_3e_2 + g_2e_3 & 2g_3e_3 \end{pmatrix},\end{aligned}$$

to denote the direction of strain. Since simple shearing keeps volume unchanged, $\boldsymbol{\varepsilon}$ is a deviatoric tensor, i.e., $\mathrm{trace}\,\boldsymbol{\varepsilon} = 0$. Thanks to the orthonormality of $\boldsymbol{e}$ and $\boldsymbol{g}$, the second basic invariant of this tensor satisfies $\varepsilon_{\mathrm{II}} = (\boldsymbol{\varepsilon} : \boldsymbol{\varepsilon})/2 = 1$. This means that $\boldsymbol{\varepsilon}$ is the deviatoric strain tensor normalized by this invariant.

In terms of the components of $\boldsymbol{\varsigma}$ and $\boldsymbol{\varepsilon}$, Eq. (13) becomes

$$\begin{aligned}\tau = -\,(&\varepsilon_{11}\varsigma_{11} + \varepsilon_{22}\varsigma_{22} + \varepsilon_{33}\varsigma_{33} \\ &+ \varepsilon_{23}\varsigma_{23} + \varepsilon_{31}\varsigma_{31} + \varepsilon_{12}\varsigma_{12})\,\lambda D.\end{aligned} \tag{16}$$

This is further simplified to the equation,

$$\tau = (\vec{\varsigma}\cdot\vec{\varepsilon})\,\lambda D \tag{17}$$

using the six-dimensional vectors,

$$\begin{aligned}\vec{\varsigma} &= \left(\frac{\varsigma_{11}}{\sqrt{2}}, \frac{\varsigma_{22}}{\sqrt{2}}, \frac{\varsigma_{33}}{\sqrt{2}}, \varsigma_{23}\,\varsigma_{31}, \varsigma_{12}\right)^{\mathrm{T}} \\ \vec{\varepsilon} &= -\left(\sqrt{2}\varepsilon_{11}, \sqrt{2}\varepsilon_{22}, \sqrt{2}\varepsilon_{33}, \varepsilon_{23}, \varepsilon_{31}, \varepsilon_{12}\right)^{\mathrm{T}}\end{aligned} \tag{18}$$

The conditions, $\varsigma_{\mathrm{II}} = 1$ and $\varepsilon_{\mathrm{II}} = 1$, yield $|\vec{\varsigma}| = 1$ and $|\vec{\varepsilon}| = 1$. That is, $\vec{\varsigma}$ and $\vec{\varepsilon}$ are unit vectors. In addition, because of $\varsigma_{11} + \varsigma_{22} + \varsigma_{33} = 0$, $\vec{\varsigma}$ has five degrees of freedom, and the same is true for $\vec{\varepsilon}$. This means that five-dimensional vectors corresponding to $\vec{\varsigma}$ and $\vec{\varepsilon}$ are enough for our theoretical analyses. However, the arbitrariness in the choice of coordinate system in the five-dimensional space gives rise to the variations in the vector components depending on researchers (e.g., Il'yushin, 1954; Ohashi et al., 1975; Kocks et al., 1983; Sato and Yamaji, 2006), and we use the five-dimensional vectors,

$$\vec{\sigma} = \begin{pmatrix} \frac{1}{2}(\varsigma_{11} - \varsigma_{33}) \\ \frac{1}{2\sqrt{3}}(-\varsigma_{11} + 2\varsigma_{22} - \varsigma_{33}) \\ \varsigma_{23} \\ \varsigma_{31} \\ \varsigma_{12} \end{pmatrix} \tag{19}$$

and

$$\vec{\epsilon} = -\begin{pmatrix} \frac{1}{2}(\varepsilon_{11} - \varepsilon_{33}) \\ \frac{2}{\sqrt{3}}(-\varepsilon_{11} + 2\varepsilon_{22} - \varepsilon_{33}) \\ \varepsilon_{23} \\ \varepsilon_{31} \\ \varepsilon_{12} \end{pmatrix},$$

which are called sigma- and epsilon-vectors, and represent, respectively, a reduced stress stress tensor and a twin or untwin datum that is represented by the pair, $\boldsymbol{e}$ and $\boldsymbol{g}$. The conditions, $\varsigma_{\mathrm{II}} = \varepsilon_{\mathrm{II}} = 1$, yield $|\vec{\sigma}| = |\vec{\epsilon}| = 1$, meaning that the endpoints of the vectors exist on the unit sphere, S, in the five-dimensional space. Hence, the vectors are identified with points on S.

S is a curved four-dimensional space. Accordingly, there are always four directions that lie on S and meet at right angles, analogous to a sphere in three-dimensional space on which there are always two directions making right angles. If the information of size is abstracted away from stress ellipsoid, the principal orientations and Φ indicate the remaining information; and the principal orientations are denoted by three angles, e.g., ϕ_1, ϕ_2 and ϕ_3 in Fig. 1a. Mutually perpendicular four directions from a point on S correspond to the changes in Φ and the three angles (Fig. 1b). If the three angles are kept constant and only Φ changes along a direction on S, it is referred to as the Φ-direction on S. If the three angles are unchanged, the variation of Φ is represented by the great circle along the Φ-direction. The planes on which the great circles lie are called π-planes in plasticity theory (e.g., Khan and Huang, 1995).

In case $\boldsymbol{\varsigma}$ is a diagonal matrix, the stress axes coincide with the coordinate axes in the physical space. Then, we have $\vec{\sigma} = (*, *, 0, 0, 0)^{\mathrm{T}}$, where $*$ stands for the components of a

two-dimensional unit vector. Therefore, sigma-vectors lying on the 12-coordinate plane in the five-dimensional space form a π-plane. The sigma-vectors lying on this plane are different only in their Φ values (Fig. 1c). The sigma-vectors with $\Phi = 0$ and 1 make the angles of the multiples of 60°. Φ changes along the great circle defined by the intersection of S and the 12-coordinate plane (Fig. 1). The antipodal points on this great circle represent the stresses that have the stress ratio, Φ and $1-\Phi$, and the reverse order of eigenvalues, e.g., $\varsigma_{33} < \varsigma_{22} < \varsigma_{11}$ and $\varsigma_{11} < \varsigma_{22} < \varsigma_{33}$. Since the orientations of the coordinate axes in the physical space are arbitrarily chosen, there is a great circle passing an arbitrary point on S along which Φ changes but the attitude of the stress ellipsoid is unchanged (Fig. 1b).

It is important for the theoretical analysis of e-twinning that the points indicated by epsilon-vectors are not distributed densely on S. Those on a π-plane exist at the point corresponding to the sigma-vectors with $\Phi = 1/2$ (Fig. 1c). This is shown as follows. The point in the five-dimensional space representing the paired data, $\boldsymbol{g} = (1, 0, 0)^{\mathrm{T}}$ and $\boldsymbol{e} = (0, 0, -1)^{\mathrm{T}}$, is $(0, 0, 0, -1, 0)$, which corresponds to

$$\boldsymbol{\varsigma} = \begin{pmatrix} 0 & 0 & 1 \\ 0 & 0 & 0 \\ 1 & 0 & 0 \end{pmatrix}.$$

This matrix has the eigenvalues, -1, 0 and 1, meaning that $\Phi = 1/2$. This statement holds not only for the pair but also for other pairs of $\boldsymbol{e}$ and $\boldsymbol{g}$ thanks to the benefit of the normalization of reduced stress and strain tensors. Since the choice of coordinate orientations is arbitrary, the statement on the specific vectors apply to other couples. Accordingly, epsilon-vectors can exist only in six directions separated by 60° on a π-plane (Fig. 1c). It should be noted that epsilon-vectors can exist continuously in the directions on S perpendicular to π-planes. The epsilon-vectors that correspond to the three twin sets of a calcite grain meet at angles of ~77° in the five-dimensional space. Therefore, the vectors are not coplanar, and do not exist on the same π-plane.

3.2. Twinning condition and yield locus

The vectors, $\vec{\sigma}$ and $\vec{\epsilon}$, are different from $\vec{\varsigma}$ and $\vec{\varepsilon}$ only in the choice of coordinate systems: They represent the same physical entities (Sato and Yamaji, 2006; Yamaji and Sato, 2006). Eq. (17) is, accordingly, rewritten as

$$\tau = (\vec{\sigma} \cdot \vec{\epsilon})\, \lambda D. \tag{20}$$

Let ψ be the angle between $\vec{\sigma}$ and $\vec{\epsilon}$. Note that $\vec{\sigma} \cdot \vec{\epsilon} = \cos\psi$ and $-1 \le \cos\psi \le 1$. It follows that $\vec{\sigma} \cdot \vec{\epsilon}$ is the orthogonal projection of $\vec{\sigma}$ onto the line parallel to $\vec{\epsilon}$ (Fig. 2). We call

$$\underline{\tau} \equiv \tau / \lambda D \tag{21}$$

as non-dimensionalized resolved shear stress.

Using Eq. (20), the condition for e-twinning in Eq. (2) is rewritten as

$$\tau_{\mathrm{c}} / \lambda D \le \vec{\sigma} \cdot \vec{\epsilon}. \tag{22}$$

It follows that twin data must satisfy $\cos\psi > \tau_{\mathrm{c}}/\lambda D$, and untwin data must satisfy $\cos\psi < \tau_{\mathrm{c}}/\lambda D$. That is, the epsilon-vectors corresponding to twin data should be in the spherical cap centered by $\vec{\sigma}$ and with the radius,

$$\Psi = \cos^{-1}(\tau_{\mathrm{c}}/\lambda D), \tag{23}$$

along the surface of S. Those corresponding to untwin data exist out of the cap. Ψ is a monotonously increasing function of D with a steep slope between 20 and ~50 MPa (Fig. 3). Ψ asymptotes to 90° for the limit, $D \to \infty$. It follows from Eq. (23) that

$$\cos\Psi = \tau_{\mathrm{c}} / \lambda D. \tag{24}$$

Let $\vec{\epsilon}_{\mathrm{t}}$ and $\vec{\epsilon}_{\mathrm{u}}$ be the epsilon-vectors corresponding to twin and untwin data, respectively. It follows from the inequality (22) that

$$(\tau_{\mathrm{c}}/\lambda)\vec{\epsilon}_{\mathrm{t}} \cdot \vec{\sigma} \le D < (\tau_{\mathrm{c}}/\lambda)\vec{\epsilon}_{\mathrm{u}} \cdot \vec{\sigma}.$$

Therefore, twin and untwin data place constraints on the lower and upper bounds of D (Fry, 2001). That is, untwin data are indispensable for the paleostress analysis of the attitudes of e-twin lamellae to deterine D.

The equation for the yield surface for e-twinning is derived as follows. To this end, we define the five-dimensional vector,

$$\vec{x} = (\lambda D)\, \vec{\sigma}. \tag{25}$$

Combining Eqs. (2) and (20), we obtain the equation for the critical condition of e-twinning,

$$\tau_{\mathrm{c}} = \vec{\epsilon} \cdot \vec{x}. \tag{26}$$

This is also an equation of a hyperplane perpendicular to $\vec{\epsilon}$ with the distance, τ_{c}, from the origin of the space (Takeshita et al., 1987; Fry, 2001). Since the possible directions of epsilon-vectors are separated by 60° on a π-plane (Fig. 1c), the hyperplanes corresponding to the epsilon-vectors define a regular hexagon on a π-plane, which defines the yield locus of e-twinning (Fig. 4a). The reason for the yield locus to have the hexagonal shape is the discrete directions of epsilon-vectors on a π-plane. Contour lines of D on a π-plane are regular hexagons as well. Epsilon-vectors are discretely distributed on a π-plane, but they can have continuous distributions in the ψ-directions on S (Fig. 4b), defining the yield surface of e-twinning. Figures 4c–f show the increase of Ψ and the stepwise replacement of the attributes of epsilon-vectors from 'untwinned' to 'twinned' with increasing D.

4. Information-theoretical evaluation of constraints

Here, we introduce information theory to quantify the constraints on stress from twin and untwin data. Suppose that a data set is compatible with a set of deviatoric stress tensors. If the variation among the elements of the latter set is small, the data set is said to place a tight constraint on stress. Then, a randomly chosen deviatoric stress tensor is compatible with the data set at a small probability. Accordingly, the measure of the constraint can be related with such a probability.

On the other hand, if a data set places tight constraints, the set has a large amount of information about stress. Therefore, the constraints can be measured by this amount. If P is the probability of a deviatoric stress tensor to be compatible with a data set, the quantity,

$$I = -\log_2 P, \tag{27}$$

is called the information content of the set (e.g., Jones and Jones, 2000), and is measured by the bit. If P is large, a data set has a low information content, and places loose constraints. It is shown in the next section that the information content of a twin datum is always greater than that of an untwin datum. And, both the information contents approach 1 bit for $D \to \infty$.

To quantify the information contents of twin and untwin data sets, let us consider the probability of a randomly chosen $\boldsymbol{T}$ with a prescribed D value to be compatible with the data set. Such a tensor corresponds to $\vec{\sigma}$. And, the random sampling is substituted by the random sampling of a point from S. S is divided into two regions. One of the regions is composed of the points that correspond to deviatoric stress tensors compatible with the data set (Fig. 5); and the points corresponding to the tensors incompatible with the data set make up the other region. The probability, P, equals the ratio of the area of the former region to S, the surface area of S. The former area can be evaluated numerically as follows.

Observe that the twinning condition in Eq. (22) is equivalent with the situation whether the function, $H(\lambda D\vec{\sigma}\cdot\vec{\epsilon}-\tau_c)$, has the value 1 or 0, where

$$H(x) = \begin{cases} 1 & (x \geq 0) \\ 0 & (x < 0), \end{cases}$$

is the Heaviside step function. In case the function has the value 1, the deviatoric stress tensor corresponding to $\lambda D\vec{\sigma}$ is compatible with the datum that is represented by $\vec{\epsilon}$. In case the function has the value 0, the tensor is incompatible with the datum. Therefore, we have the probability of randomly chosen deviatoric stress tensor to be compatible with the datum,

$$P_t(D) = \frac{1}{S}\int_S H(\lambda D\vec{\sigma}\cdot\vec{\epsilon}-\tau_c)\,\mathrm{d}S, \tag{28}$$

in which $\vec{\sigma}$ is the variable of integration. This equation denotes the probability for randomly chosen deviatoric stress tensors that is represented by $\lambda D\vec{\sigma}$ to be compatible with the datum that is represented by $\vec{\epsilon}$. This integration was evaluated numerically using the set of a great number of points, $C = \{\vec{c}^{(1)}, \vec{c}^{(2)}, \ldots, \vec{c}^{(M)}\}$, which were distributed with uniform intervals over S (Fig. 5). That is, $\vec{\sigma}$ can be replaced with the elements of this set, and the integration is replaced with summation. As a result, we have

$$P_t(D) \approx \frac{1}{M}\sum_{m=1}^{M} H(\lambda D\vec{c}^{(m)}\cdot\vec{\epsilon}-\tau_c). \tag{29}$$

Such a convenient set of objects that allows us to replace a definite integral with the summation of the function values is known as a low-discrepancy sequence, which is used in mathematical finance (Drmota and Tichy, 1997). Without loss of generality, we can assume $\boldsymbol{e} = (0, 0, -1)^{\mathrm{T}}$ and $\boldsymbol{g} = (1, 0, 0)^{\mathrm{T}}$ to evaluate the information contents of a twin and an untwin datum. It follows that $\vec{\epsilon} = (0, 0, 0, 1, 0)^{\mathrm{T}}$. Then, Eq. (29) becomes

$$P_t(D) \approx \frac{1}{M}\sum_{m=1}^{M} H(c_4^{(m)}\lambda D-\tau_c), \tag{30}$$

where $c_4^{(m)}$ is the fourth component of $\vec{c}^{(m)}$. Substituting this into Eq. (27), we obtain the information content of a twin datum,

$$I_t(D) \approx \log_2 M - \log_2 \sum_{m=1}^{M} H(c_4^{(m)}\lambda D-\tau_c). \tag{31}$$

Likewise, we obtain that of an untwin datum,

$$I_u(D) \approx \log_2 M - \log_2 \sum_{m=1}^{M} H(\tau_c - c_4^{(m)}\lambda D). \tag{32}$$

The summation in Eq. (31) indicates the number of points in C where the condition, $\tau \geq \tau_c$, is satisfied.

Eq. (31) indicates that the information content of a twin datum depends on D. $I_t(D)$ denotes the information content of a twin set that was formed at the differential stress. And, I_u denotes the information content of a twin set that was left untwinned at the differential stress. However, when we study paleo stresses, we do not know the differential stress at which e-twins were formed. Then, $I_t(D)$ indicates the information content of a twin set that was formed at an *assumed* differential stress. Such measures may seem useless, but they are shown to be useful in the following sections of this paper especially in the stress inversion of twin data.

In this study, we used the 60,000 points on S, which were generated by Yamaji and Sato (2012), to calculate information contents, i.e., $M = 60,000$. In addition, the points were used in the following part of this paper as the trial stress tensors, each of which is tested whether it explains twin data.

5. Constraints from twin and untwin data

The constraints of twin and untwin data are evaluated in this section. The contents at very low and very high stress levels are easily evaluated. It is clear that twinning does not occur when $D < 2\tau_c$. In this case, we have $I_u(D) = 0$, because any stress with $D < 2\tau_c$ explains an untwin datum. And, $I_t(D)$ is not defined, because $P_t(D) = 0$. On the other hand, the twinning condition (Eq. 22) approaches

$$\vec{\sigma}\cdot\vec{\epsilon} \geq 0. \tag{33}$$

for $D \to \infty$. This inequality indicates the hemisphere centered by $\vec{\epsilon}$. It follows that both P_t and P_u asymptote to 1/2, and so $I_t(\infty) = I_u(\infty) = 1$ bit.

The information contents at intermediate D values were numerically evaluated using Eqs. (31) and (32). The information content of (or the constraint from) a twin datum was always

greater than that of an untwin datum (Fig. 6), meaning that a twin datum is more valuable than an untwin datum. If the D value at the time of twinning was smaller than ~100 MPa, the constraint from a twin datum was ~10 to several times more significant than that from an untwin datum. If the D value was greater than ~100 MPa, they were comparably significant.

Paired stereograms in Fig. 7 shows the stresses with various D values that are compatible with a twin and an untwin data with the vertical $\boldsymbol{e}$ and eastward $\boldsymbol{g}$. Corresponding to the monotonous increase of $I_t(D)$, the stresses compatible with a twin datum increase their variation with increasing D. Note that the patterns in the paired stereoplots with $D = 50$ and 1000 MPa have tiny difference. Figure 6 shows that the increase of the information content of a twin datum become gentle at around 100 MPa. Therefore, the paleostress analysis of the orientations of twin data loses resolution for differential stresses if twin lamellae were formed at differential stress greater than 50–100 MPa. In contrast, variation of the stresses compatible with the untwin datum changes slowly when D is of the order of 10^1 MPa, and continues to change beyond 100 MPa. Untwin data are important to place the upper bound on the differential stresses in paleo stress determination from e-twins. Green is a dominant color in Fig. 7. This is a result of the fact that stress ratio tends to have intermediate values: It is a natural feature of a uniform distribution of stress tensors that triaxial stresses with intermediate Φ values are abundant and that axial stresses ($\Phi \approx 0$ or 1) are rare (Sato and Yamaji, 2006).

6. Constraints from n-plets

6.1. The minimum differential stresses for generating n-plets

The minimum differential stress for e-twinning is $2\tau_c$. Obviously, the minimum one for singlet to be formed is also $2\tau_c$: The occurrence of singlet places the constraint on the minimum differential stress (Fig. 8a). Do doublet and triplet have the same threshold? It seems that the minimum one for n-plet has positive correlation with n, because the condition, $\tau \geq \tau_c$, must be met simultaneously on e-planes this different orientations. The minimum ones were determined theoretically as follows.

Doublet. Suppose that doublets are formed only in the optimally oriented calcite grains, and that those grains have vertical c-axes and a westerly dipping untwinned plane (Fig. 8b). From the symmetry of the crystal structure and that of stress tensor, it is obvious that the stress tensor allowing twinning only on the remaining e-planes has the σ_1- and σ_3-axes lying on the E-W trending vertical plane. It can been seen (Appendix A) that doublet is formed at the minimum differential stress with $\Phi = 1$ and the westward dip of the $\sigma_1\sigma_2$-plane,

$$p = \frac{1}{2}\tan^{-1}\left(\frac{4\cos 2\alpha}{5\sin 2\alpha}\right). \tag{34}$$

It follows from $\alpha = 26.25°$ that $p \approx 15.7°$, and from and Eqs. (A.2) and (A.3) that the minimum differential stress is approximately equal to $2.27\tau_c$. If $\tau_c = 10$ MPa, the occurrence of doublet indicates differential stress greater than 22.7 MPa.

Triplet. From the symmetries of stress tensor (orthorhombic or axial) and of the configuration of the e-planes and their gliding directions of a triplet, it is obvious that the minimum stress to generate a triplet is axial tension ($\Phi = 1$) with the σ_3-axis parallel to the c-axes of the triplets (Fig. 8c). Substituting $p = 0$ into Eq. (A.2), we obtain $\tau = (1/2)\sin 2\alpha$. Therefore, we have the smallest differential stress, $D_{\min} = (2/\sin 2\alpha)\tau_c \approx 2.52\tau_c$, for generating triplets. If $\tau_c = 10$ MPa, the occurrence of triplet indicates the differential stress greater than 25.2 MPa.

6.2. Information contents and compatible stresses for n-plates

The information contents of n-plets were calculated as a function of D using the computational grid, $\left\{\vec{c}^{(1)}, \vec{c}^{(2)}, \ldots, \vec{c}^{(60000)}\right\}$. $I_n(D)$ refers to the content of the n-plet. The results are shown in Fig. 9. Since no twinning occurs when $D < 2\tau_c$, we have $I_0(D < 2\tau_c) = 1$. $I_0(D)$ shows a gradual increase in the range, $2\tau_c \leq D$.

Corresponding to the minimum differential stresses of singlet, doublet and triplet, $I_1(D \leq 2\tau_c)$, $I_2(D \leq 2.3\tau_c)$ and $I_3(D \leq 2.5\tau_c)$ have no value. $I_1(D)$, $I_2(D)$ and $I_3(D)$ decrease rapidly in the range, $D \lesssim 50$ MPa. It is clear from Fig. 9 that the constraints from n-plets become tighter with increasing n. And, constraint from a zeroplet becomes more important than those from singlet and doublet for $D \gtrsim 70$ and 150 MPa, respectively, if τ_c is 10 MPa.

Fig. 9 also shows the convergence, $I_1(\infty) = I_2(\infty) \approx 1.6$ bits, and $I_3(\infty) = I_0(\infty) \approx 2.5$ bits. The relationship, $I_1(\infty) = I_2(\infty) < I_3(\infty) = I_0(\infty)$, can be theoretically derived as well. To this end, let $\vec{\epsilon}^{(1)}$, $\vec{\epsilon}^{(2)}$ and $\vec{\epsilon}^{(3)}$ be the sigma-vectors of the three twin sets of a calcite grain. It follows from Eq. (33) that the sigma-vectors satisfy the simultaneous inequalities,

$$\vec{\epsilon}^{(1)}\cdot\vec{\sigma} < 0,\ \vec{\epsilon}^{(2)}\cdot\vec{\sigma} < 0,\ \vec{\epsilon}^{(3)}\cdot\vec{\sigma} < 0 \quad \text{for zeroplet} \tag{35}$$

$$\vec{\epsilon}^{(1)}\cdot\vec{\sigma} \geq 0,\ \vec{\epsilon}^{(2)}\cdot\vec{\sigma} < 0,\ \vec{\epsilon}^{(3)}\cdot\vec{\sigma} < 0 \quad \text{for singlet} \tag{36}$$

$$\vec{\epsilon}^{(1)}\cdot\vec{\sigma} \geq 0,\ \vec{\epsilon}^{(2)}\cdot\vec{\sigma} \geq 0,\ \vec{\epsilon}^{(3)}\cdot\vec{\sigma} < 0 \quad \text{for doublet} \tag{37}$$

$$\vec{\epsilon}^{(1)}\cdot\vec{\sigma} \geq 0,\ \vec{\epsilon}^{(2)}\cdot\vec{\sigma} \geq 0,\ \vec{\epsilon}^{(3)}\cdot\vec{\sigma} \geq 0 \quad \text{for triplet} \tag{38}$$

at the limit, $D \to \infty$. Obviously, if $\vec{\sigma}$ is a solution of the simultaneous inequalities in (35), $-\vec{\sigma}$ is a solution of those in (38). It follows that $I_0(\infty) = I_3(\infty)$. Likewise, we obtain $I_1(\infty) = I_2(\infty)$ from the inequalities in (36) and (37).

The stresses compatible with n-plets are illustrated as the functions of D in Fig. 10. The information contents of a singlet, doublet and triplet show rapid declines in the range, $D \lesssim 50$ MPa (Fig. 9), and compatible stresses show rapid changes as well (Fig. 10). Consequently, singlets, doublets and triplets places tight constraints on stress stress magnitudes at low stress levels.

If sigma-vectors are antipodal to each other, i.e., $\vec{\sigma}$ and $-\vec{\sigma}$, the corresponding deviatoric stress tensors are different only in sign, i.e., $\boldsymbol{T}$ and $-\boldsymbol{T}$, called opposite stresses. Accordingly, the complementary relationship of the simultaneous inequalities (35) and (38) results in their solutions to be opposite stresses. This is reflected by the opposite patterns in the stereograms of the compatible stresses of a zeroplet and triplet at $D = 1000$

MPa in Fig. 10. The complementary relationship of the simultaneous inequalities (36) and (37) results in the opposite patterns in the stereograms of a singet and doublet at $D = 1000$ MPa as well.

The constraint from a twin datum is smaller than those from a doublet and a triplet (Figs. 6 and 9). Hence, the discrimination of n-plets places constraints on stress more tightly than the simple summation of the constraints from twin and untwin data. However, paleostress analysis based on this discrimination is weak to the sampling bias, which is considered in the next section.

7. Sampling bias

The importance of untwin datum to constrain the upper bound of D and of the discrimination of n-plets was considered in the previous sections by means of their information contents. However, the existence of what you observe is certain, but the nonexistence of what you do not observe is not. Twin lamellae subparallel to the thin section are hardly observed especially in calcite grains with small twin densities, but those perpendicular to the section are easily observed. This bias may have a distortive effect to the stress and strain analyses of e-twin lamellae. A twin set is misclassified as untwinned one by this bias.

The chance to observe a twin lamella increases with the increasing angle between the lamella and the thin section. It is affected by the number density of twin lamellae as well. The experimental study by Rybacki et al. (2013) showed that the density is 10–100 twins/mm for differential stresses of the order of 10–100 MPa. E-twin data were collected from calcite grains with the grain sizes of a few hundred microns (e.g., Turner et al., 1954; Lacombe and Laurent, 1996; Rocher et al., 2004). Thus, the bias can be serious to determine stress from calcite with low twin densities. Though the bias depends not only on the angle but also on the number density and width of twin lamellae, we concentrate our attention to the geometric factor of the bias. The probability for the lamella to be observed is proportional to $\sin\chi$ (Terzaghi, 1965), where χ is the angle between a twin lamella and the thin section, and the constant of proportionality depends on twin spacing, width, etc. However, we assign the probability, $\sin\chi$, for simplicity to the validity for a potential twin plane to be judged untwinned.

To assess the bias, artificial data sets were generated as follows. First, ten thousand calcite grains were assumed to have isotropic lattice fabric: The a- and c-axes were randomly oriented. Since stresses tend to have intermediate stress ratios (Lisle et al., 2006; Sato and Yamaji, 2006), triaxial stresses with $\Phi = 0.5$ were applied to the hypothetical calcite aggregate with differential stresses from 30 to 480 MPa. And, it was judged whether the condition, $\tau \geq \tau_c$, was met on each of the three twin planes of the grains. Since the principal orientations do not affect the sampling bias, $\boldsymbol{Q}$ was assumed to be equal with $\boldsymbol{I}$ in Eq. (4). As a result, each plane got the attribute, 'twinned' or 'untwinned.' In this way unbiased data sets were generated. Finally, to generate biased data sets, the attribute, 'twinned,' was exchanged with 'untwinned' for randomly chosen twinned planes with the probability of $1 - \sin\chi$ to simulate misclassification by the sampling bias. Fig. 11 shows the results.

The ratio of twinned and untwinned planes increases with increasing D. The numerical experiment showed that the 20–25% of twin planes were overlooked by the bias (Fig. 11a), and that this percentage was relatively insensitive to D. The twinning incidence is the percentage of grains including twin lamellae. The positive correlation of this parameter with D was used to determine differential stress (Rowe and Rutter, 1990).

The percentages of grains with $n = 0$, 1, 2 and 3 are significantly affected by the bias (Fig. 11c). Figure 11d shows the error rate in the classification of n-plets. The error rate is defined as $(m - m')/m$, where m and m' are the numbers of n-plets in the unbiased and biased cases, respectively. The bias resulted in the overestimation of the number of zeroplets, and the error rate of zeroplet increased 6 to 92% with increasing D from 30 to 480 MPa. The bias diminished the numbers of singlets, doublets and triplets. Their error rates were 15–30% for $D \gtrsim 50$ MPa. When D was smaller than ~50 MPa, the error rates of doublets and triplets were statistically unstable, because doublets and especially triplets were rare at low stress levels. At the worst, the error rate reached −40%.

8. Discussion

In the first place, do calcite e-twins constrain stress or strain? Paleostress analysis using calcite e-twins received criticism in that they inherently indicate strain rather than stress (e.g., Groshong, 1972; Groshong et al., 1984). Indeed, e-twinning leads to a simple shear of the calcite grain that hosts the twin lamellae (Fig. 1a) (e.g., Groshong, 1972). The strain analysis of the twin lamellae may be relatively robust to the sampling bias, because twin sets with low number densities are overlooked more often than those with high number densities. The former sets represent strains smaller than the latter ones.

However, there are three-dimensional strains that cannot be achieved by the simple shear on the three twin planes, because simple shearing on at least five planes with different orientations are necessary to achieve arbitrary strain (Reid, 1973, p. 148). For example, shortening along the c-axis cannot be accommodated by e-twinning. It follows that strain compatibility across grain boundaries is not guaranteed for e-twinning. Strain field in polycrystalline calcite is heterogeneous (Venkitasubramanyan, 1971; Spiers, 1979; Burkhard, 1993). It is not theoretically but empirically supported that the microscopic strains evaluated from twins represent macroscopic tectonic deformations (e.g., Groshong et al., 1984; Evans and Dunne, 1991). On the other hand, it was demonstrated empirically that the results of stress inversion of calcite twin data fault-slip data coincide satisfactorily (Lacombe et al., 1990, 1992). The methodology of stress inversion of calcite twin and untwin data should be pursued.

The constraints from twin and untwin data of calcite e-planes were measured in this work by means of information contents. The evaluation was enabled by the fact that the five-dimensional stress space was defined to fulfill the principle of coordinate invariance (e.g., Ottosen and Ristinmaa, 2005): Physical laws

must be formulated in mathematical forms that are independent from the choice of a coordinate system. As a result, the choice does not affect geometrical properties including angles and distances in the five-dimensional space. Fry (2001) was a breakthrough paper in that he presented the geometrical interpretation of the condition of calcite e-twinning, but his stress space did not fulfill the principle.

The information contents of doublet and triplet are larger than those of twinned and untwinned e-planes (Figs. 6 and 9). It means that constraints from doublets and triplets are tighter than those of twin and untwin data. In addition, the gradient of the information content of triplet, $\mathrm{d}I/\mathrm{d}D$, declines rapidly when D is smaller than ~100 MPa and gradually when D is in the range $100 \lesssim D \lesssim 200$ MPa. Therefore, doublets and triplets can determine differential stress better than twinned and untwinned e-planes. However, it is difficult to classify n-plets accurately due to the sampling bias (Fig. 11).

Differential stress has been estimated from the twin incidence and from the relative percentages of grains twinned on 0, 1, 2 or 3 twin planes. However, such parameters are inevitably affected by the sampling bias to some extent. At the worst case this classification has the error rates of 20–30%, corresponding roughly to the uncertainty of 0.01–0.15 in Jamison and Spang's (1976) S_1 parameter, which gives rise to the underestimation of D by a factor of ~1/2 (Jamison and Spang, 1976, Eq. 3). The bias resulted also in the decrease of twin incidence by 5–17 points (Fig. 11b), giving rise to the underestimation of D by 10–36 MPa according to Eq. (1) of Rowe and Rutter (1990). Twin and untwin data loose resolution in D if twin lamellae are formed under stress conditions with D greater than 50–100 MPa. Hence the bias can give rise to a serious error in determining differential stress. It was shown in §6.1 that doublet and triplet are formed at their minimum D with $\Phi = 1$. However, Jamison and Spang (1976) assumed $\Phi = 0$ to estimate D, resulting in inaccuracy to some extent.

The assumption, $\Phi = 0$, allowed Jamison and Spang (1976) to evaluate the percentages of n-plets as the functions of D by measuring the areas of the regions on a unit sphere in three-dimensional space. That is, since they assumed axial compression, reduced stress tensor had two degrees of freedom to denote the σ_1-orientation, which was identified with a point on the sphere. So, the variation in the orientation compatible with an n-plet was represented by the area. If they did not assume a value of Φ, they had to define the unit sphere in the five-dimensional stress space, S. In this respect, the arguments using information contents in this paper is an extension of their work, and the extension was enabled by the principle of coordinate invariance.

Paleostresses have been estimated from twinned/untwinned e-planes, twin incidence, and the percentages of n-plets, but these ratios are easily affected by the sampling bias at differential stresses greater than ~100 MPa. This is evidenced by the graphs in Figs. 11a–c. That is, the gradients of the graphs asymptote to zero with increasing D, meaning that a small perturbation in the ratio (the ordinate of the graph) results in a large perturbation in D (the abscissa). All the ratios are based on the determination whether e-planes are twinned or not. This discrimination is naturally affected by the bias. Therefore, it is important to incorporate not only the determination but also the orientations of e-planes for the paleostress analysis of calcite e-twins.

9. Conclusions

The yield condition and yield locus of e-twinning were obtained using the five-dimensional stress space, which satisfies the principle of coordinate invariance.

The constraints from twinned and untwinned e-planes and from n-plets were measured by their information contents. Not only twin but also untwin data are necessary to determine D, but it was found that the constraints of untwin data are much looser than those of twin data. The constraints of singlet, double and triplet become tighter in this order. The constraint of zeroplet is looser than twinned grains at low differential stresses, but becomes tigher than singlet and doublet at D greater than $\sim 7.5\tau_c$ and $\sim 15.0\tau_c$, respectively. The existence of doublet and triplet places the constraints on the lower bound of D at $2.27\tau_c$ and $2.52\tau_c$, respectively. E-twin lamellae loose the resolution of D if they were formed under the condition, $D \gtrsim 10\tau_c$.

At the worst 25% of twin lamellae are overlooked due to sampling bias, which gives rise to the misclassification of n-plets. Especially, triplets tend to be misclassified into doublets and singlets. Accordingly, the determination of stress magnitude using the classification appears inaccurate. The bias gives distortive effect to the estimation of D using the discrimination of twinned/untwinned e-planes when twins were formed at D greater than $\sim 10\tau_c$.

Acknowledgments

I thank Dr. O. Nishikawa for discussions. The author is grateful to Prof. O. Lacombe and Dr. J. Sippel for helpful comments to an early version of this paper, which improved the manuscript.

Appendix A. Minimum differential stress for doublet

The minimum differential stress, $D_{\min}$, required for forming doublet is determined as follows. Suppose that doublets are formed only in the optimally oriented calcite grains with vertical c-axes and untwinned planes with easterly $\boldsymbol{e}$-vectors (Fig. 8b). Now, consider the right-handed, rectangular Cartesian coordinates with the eastward and northward pointing first and second coordinate axes and the vertical third axis. Then, the twinned plane has

$$\begin{aligned} \boldsymbol{e} &= (\sin\alpha\cos 120^\circ, \pm\sin\alpha\sin 120^\circ, -\cos\alpha)^{\mathrm{T}} \\ \boldsymbol{g} &= (\cos\alpha\cos 120^\circ, \pm\cos\alpha\sin 120^\circ, \sin\alpha)^{\mathrm{T}}. \end{aligned} \tag{A.1}$$

From the symmetry of the crystal structure and that of stress tensor, it is obvious that the stress tensor allowing twinning only on the planes has the σ_1- and σ_3-axes lying on the E-W trending

vertical plane. It follows from Eq. (4) that the stress tensor of this case is represented by

$$\boldsymbol{\sigma} = \frac{1}{2}\begin{pmatrix} 1+\cos 2p & 0 & \sin 2p \\ 0 & \Phi & 0 \\ \sin 2p & 0 & 1-\sin 2p \end{pmatrix} D.$$

where p denotes the westward plunge of the σ_1-axis. This tensor has the principal stresses, 0, $D\Phi$ and D. Under this stress condition, the resolved shear stress on the twinned plane along the gliding direction (Eq. A.1) has the expression,

$$\tau_c = f(p) D_{\min}, \tag{A.2}$$

with

$$f(p) = \frac{1}{16}(5\sin 2\alpha \cos 2p - 3\sin 2\alpha + 4\cos 2\alpha \sin 2p + 6\Phi \sin 2\alpha). \tag{A.3}$$

Since the left-hand side of Eq. (A.2) is a constant, Eq. (A.2) holds for the p value that maximizes $f(p)$. It is necessary for this maximization that $\Phi = 1$, because the coefficient of Φ in Eq. (A.3) is positive in sign. Substituting $\Phi = 1$ into Eq. (A.3), and solving $f'(p) = 0$, we obtain Eq. (34), which gives the optimal p value that allows the formation of doublets at the minimum differential stress. Once this optimal value is obtained, $D_{\min}$ is calculated by Eqs. (A.2) and (A.3).

References

Burkhard, M., 1993. Calcite twins, their geometry, appearance and significance as stress-strain markers and indicators of tectonic regime: A review. Journal of Structural Geology 15, 351–368.

Constantin, J., Laurent, P., Vergély, P., Gabrera, J., 2007. Paleo-deviatoric stress magnitudes from calcite twins and related structural permeability evolution in minor faults: Example from the toarcian shale of the French Causses Basin, Aveyron, France. Tectonophysics 429, 79–97.

Drmota, M., Ticky, R.F., 1997. Sequences, Discrepancies and Applications. Springer, Berlin.

Etchecopar, A., 1984. Etude des états de contrainte en tectonique cassante et simulation de déformations plastiques (approche mathématique). PhD Thesis, Univ. Montpellier.

Evans, M.A., Dunne, M., 1991. Strain factorization and partitioning in the North Mountain thrust sheet, central Appalachians, U.S.A. Journal of Structural Geology 13, 21–35.

Fry, N., 2001. Stress space: Striated faults, deformation twins, and their constraints on paleostress. Journal of Structural Geology 23, 1–9.

Groshong, R.H., 1972. Strain calculated from twinning in calcite. Geological Society of America Bulletin 83, 2025–2038.

Groshong, R.H., Teuffel, L.W., Gasteiger, C., 1984. Precision and accuracy of the calcite strain-gauge calculation using twinned calcite. Geolocial Society of America Bulletin 95, 357–363.

Hill, R., 1998. The Mathematical Theory of Plasticity. Clarendon Press, New York.

Il'yushin, A.A., 1954. On a connection between stresses and small strains in the mechanicsof continuous media. Prikladnaya Matematika i Mechanika 18, 641–666.

Jamison, R.W., Spang, J., 1976. Use of calcite twin lamellae to infer differential stresses. Geolgical Society of America Bulletin 87, 868–887.

Jones, G.A., Jones, M.J., 2000. Information and coding theory. Springer, London.

Khan, A.S., Huang, S., 1995. Continuum theory of plasticity. John Wiley & Sons, New York.

Kocks, U.F., Canova, G.R., Jonas, J.J., 1983. Yield vectors in f.c.c. crystals. Acta Metallurgica 31, 1243–1252.

Lacombe, O., 2007. Comparison of paleostress magnitudes from calcite twins with contemporary stress magnitudes and frictional sliding criteria in the continental crust: Mechanical implications. Journal of Structural Geology 29, 86–99.

Lacombe, O., 2010. Calcite Twins, a Tool for Tectonic Studies in Thrust Belts and Stable Orogenic Forelands. Oil & Gas Science 65, 809–838.

Lacombe, O., Angelier, J., Laurent, P., 1992. Determining paleostress orientations from faults and calcite twins: a case study near the Sainte-Victoire Range (southern France). Tectonophysics 201, 141–156.

Lacombe, O., Anglier, J., Laurent, P., Bergerat, F., Tourneret, C., 1990. Joint analysis of calcite twins and fault slips as a key for deciphering polyphase tectonics: Burgundy as a case study. Tectonophysics 182, 279–300.

Lacombe, O., Laurent, P., 1996. Determination of deviatoric stress tensors based on inversion of calcite twin data from experimentally deformed monophase samples: preliminary results. Tectonophysics 255, 189–202.

Lacombe, O., Malandain, J., Vilasi, N., Amrough, K., Roure, F., 2009. From paleostresses to paleoburial in fold-thrust belts: Preliminary results from calcite twin analysis in the Outer Albanides. Tectonophysics 475, 128–141.

Laurent, P., Bernard, P., Vasseur, G., Etchecopar, A., 1981. Stress tensor determination from the study of e twins in calcite: A linear programming method. Tectonophysics 78, 651–660.

Laurent, P., Tourneret, C., Laborde, O., 1990. Determining deviatoric stress tensors from calcite twins: Applications to monophased synthetic and natural polycrystals. Tectonics 9, 379–389.

Lisle, R.J., Orife, T.O., Arlegui, L., Liesa, C., Srivastava, D.C., 2006. Favoured states of palaeostress in the Earth's crust: evidence from fault-slip data. Journal of Structural Geology 28, 1051–1066.

Meyer, C.D., 2000. Matrix Analysis and Applied Linear Algebra. SIAM, Philadelphia.

Ohashi, Y., Tokuda, M., Yamashita, H., 1975. Effect of third invariant of stress deviator on plastic deformation of mild steel. Journal of Mechanics and Physics of Solids 23, 295–323.

Ottosen, N.S., Ristinmaa, M., 2005. The Mechanics of Constitutive modeling. Elsevier, Amsterdam.

Pfiffner, O. A., Burkhard, M. 1987. Determination of paleo-stress axes orientations from fault, twin and earthquake data. Annales Tectonicae 1, 48–57.

Reid, C.N., 1973. Deformation Geometry for Materials Scientists. Pergamon Press, Oxford.

Rocher, M., Cushing, M.,Lemeille, F., Lozac'h, Y. Angelier, J., 2004. Intraplate paleostresses reconstructed with calcite twinning and fulting: Improved method and application to the eastern Paris Basin (Lorraine, France). Tectonophysics 387, 1–21.

Rowe K.J., Rutter E.H., 1990. Paleostress estimation using calcite twinning: Experimental calibration and application to nature. Journal of Structural Geology 12, 1–17.

Rybacki, E., Evans, B., Janssen, C., Wirth, R., Dresen, G., 2013. Influence of stress, temperature, and strain on calcite twins constrained by deformation experiments. Tectonophysics 601, 20–36.

Sato, K., Yamaji, A., 2006. Embedding stress difference in parameter space for stress tensor inversion. Journal of Structural Geology 28, 957–971.

Spiers, C.J., 1979. Fabric development in calcite polycrystals deformed at 400°C. Bulletin de Minéralogie 102, 282–289.

Takeshita, T., Tomé, C., Wenk, H.-R., Kocks, U.F., 1987. Single-crystal yield surface for trigonal lattices: Application to texture transitions in calcite polycrystals. Journal of Geophysical Resarch 92, 12917–12930.

Terzaghi, R.D., 1965. Source of error in joint surveys. Geotéchnique 15, 287–304.

Tourneret, C., Laurent, P., 1990. Paleo-stress orientations from calcite twins in the North Pyrenean foreland, determined by the Etchecopar inverse method. Tectonophysics 180, 287–302.

Turner, F.J., 1953. Nature and dynamic interpretation of deformation lamellae in calcite of three marbles. American Journal of Science 251, 276–298.

Turner, F.J., Griggs, D.T., Heard, H., 1954. Experimental deformation of calcite crystals. Geological Society of America Bulletin 65, 883–934.

Twiss, R.J., Moores, E.M., 2006. Structural Geology, 2nd Edition. Freeman, New York.

Venkitasubramanyan, C.S., 1971. Qualitative analysis of three-dimensional strain using twins in calcite and dolomite. Tectonophysics 11, 217–231.

Yamaji, A., 2007. Introduction to Tectonophysics: Theoretical Aspects of Structural Geology. Terrapub, Tokyo.

Yamaji, A., Sato, K., 2006. Distances for the solutions of stress tensor inver-

sion in relation to misfit angles that accompany the solutions. Geophysical Journal International 167, 933–942.
Yamaji, A., Sato, K., 2012. A spherical code and stress tensor inversion. Computers & Geosciences 38, 164–167.

Figure and Table Captions

Fig. 1. (a) Schematic illustration of a stress ellipsoid. The size, shape and attitude of the ellipsoid are described by, D, Φ, and the angles, ϕ_1, ϕ_2 and ϕ_3, about the coordinate axes. (b) There are four directions making right angles at every point on S corresponding to the changes in the four parameters, Φ, ϕ_1, ϕ_2 and ϕ_3. (c) The section of S along the 12-coordinate plane (thick line). Stars indicate the points where $\Phi = 1/2$. Epsilon-vectors exist only at the latter points.

Fig. 2. (a) Schematic illustration showing a sigma-vector (thick solid arrow) in the five-dimensional parameter space. Thick line depicts a unit sphere. Solid and open circles on the thick line indicate the endpoints of the epsilon vectors corresponding to twin and untwin datum, respectively. Dashed line indicates the hyperplane perpendicular to $\vec{\sigma}$ at the distance, $\tau_c/\lambda D$, from the origin of the stress space, O. (b) Orthogonal projection of the endpoints of the epsilon-vectors onto the line parallel to the sigma-vector.

Fig. 3. Ψ versus D for the three cases, $\Phi = 0$, 1/2 and 1. These graphs are described by Eq. (23). The graph for other Φ values are plotted between these lines. Open circle in the inset indicates the intersection of the graph for $\Phi = 1/2$ and the horizontal line $\Psi = 30^\circ$ at $D \approx 2.3\tau_c$. Here, the critical value,$\tau_c = 10$ MPa, is assumed.

Fig. 4. (a) The regular hexagon illustrating the yield locus of e-twinning, i.e., the intersection of the yield surface and the π-plane. In this case, the plane is parallel to the 12-coordinate plane of the five-dimensional space. Thick line in the hexagon depicts the intersection of S and the plane. The endpoints of epsilon-vectors can exist at the points indicated by stars. Open circles on the hexagon is the intersection of the hexagon and the rays through the points. Φ changes linearly along the sides of the hexagon. (b) An analogue of S for illustrating the compatibility of a sigma-vector (solid circle) and epsilon-vectors. Closed stars indicate epsilon-vectors in the spherical cap centered by the sigma-vector. Open stars indicate epsilon-vectors out of the cap. Stars make lines along the ϕ_1-, ϕ_2-, ϕ_3-directions, which makes right angles with each other (Fig. 1c), but a direction perpendicular to a π-plane is illustrated here. (c–f) Replacement of untwin data by twin ones through increasing D. Both open and close circles indicate the midpoints of the sides of the hexagon in (a).

Fig. 5. Schematic illustration for the region on S, which is defined as the set of the sigma-vectors that compatible with a given data set. Open circles depict the points represented by $\vec{c}^{(1)}, \ldots, \vec{c}^{(M)}$, which are placed with regular intervals on S. P in Eq. (27) equals the ratio of the area of this region and S. And, the right-hand side of Eq. (28) is approximated by the ratio of the number of the vectors in the region and M. This is denoted by Eq. (29).

Fig. 6. Probability, P, for a randomly chosen stress with a specific D value to be compatible with a twin or an untwin datum, and their information contents, The threshold, $\tau_c = 10$ MPa, was assumed to obtain the P and I values.

Fig. 7. (a) Stereogram illustrating the assumed horizontal e-twin plane with the pole, $\boldsymbol{e}$, and its eastward gliding direction of the upper block, $\boldsymbol{g}$. (b) Paired stereograms (lower hemisphere, equal-area) indicating the stresses compatible with the twin and untwin datum shown in (a). The heads of tadpole-like symbols in the left stereogram indicate their σ_1-directions, whereas the tails of the symbols point the corresponding σ_3-axes. The heads and tails of tadpole-like symbols in the right stereogram have the opposite roles. Stress ratios are depicted by rainbow colors. Differential stresses are shown under the pairs, where the value, $\tau_c = 10$ MPa, was assumed. (For interpretation of the references to color in this figure legend, the reader is referred to the web version of this article.)

Fig. 8. Lower-hemisphere, equal-angle projections showing the stress conditions with the smallest differential stresses, $D_{\min}$, required to form singlets, doublets and triplets, the c-axes of which are assumed to be vertically oriented. Thin white arrows indicate the gliding directions. Color code and white arrow indicate the $|\tau|$ and $-\boldsymbol{s}$ directions on planes with various orientations, respectively. The stress condition with $\Phi = 0.5$ is shown in (a), but singlet can be formed at the minimum one regardless of Φ as long as both the σ_1- and σ_3-axes meet the twinned e-plane at 45°.

Fig. 9. The information contents of n-plets.

Fig. 10. Lower-hemisphere, equal-area projections showing n-plets with vertical c-axis and the stresses compatible with them for several D values. The critical resolved shear stress, τ_c, is assumed to be 10 MPa. (For interpretation of the references to color in this figure legend, the reader is referred to the web version of this article.)

Fig. 11. Sampling bias estimated using artificial data sets. (a) Ratio of the numbers of twinned and all twin sets. (b) Twinning incidence. (c) The percentages of n-plets. Solid and dotted lines indicate the percentages in the unbiased and biased cases, respectively. (d) Misclassification ratio of n-plets. If m and m' are the number of true and biased number of n-plets, this ratio is defined as $(m' - m)/m$.

Table 1. List of symbols. Vectors in the physical space and five-dimensional space are denoted by boldface letters and arrows, respective, such that $\boldsymbol{g}$ and $\vec{\sigma}$.

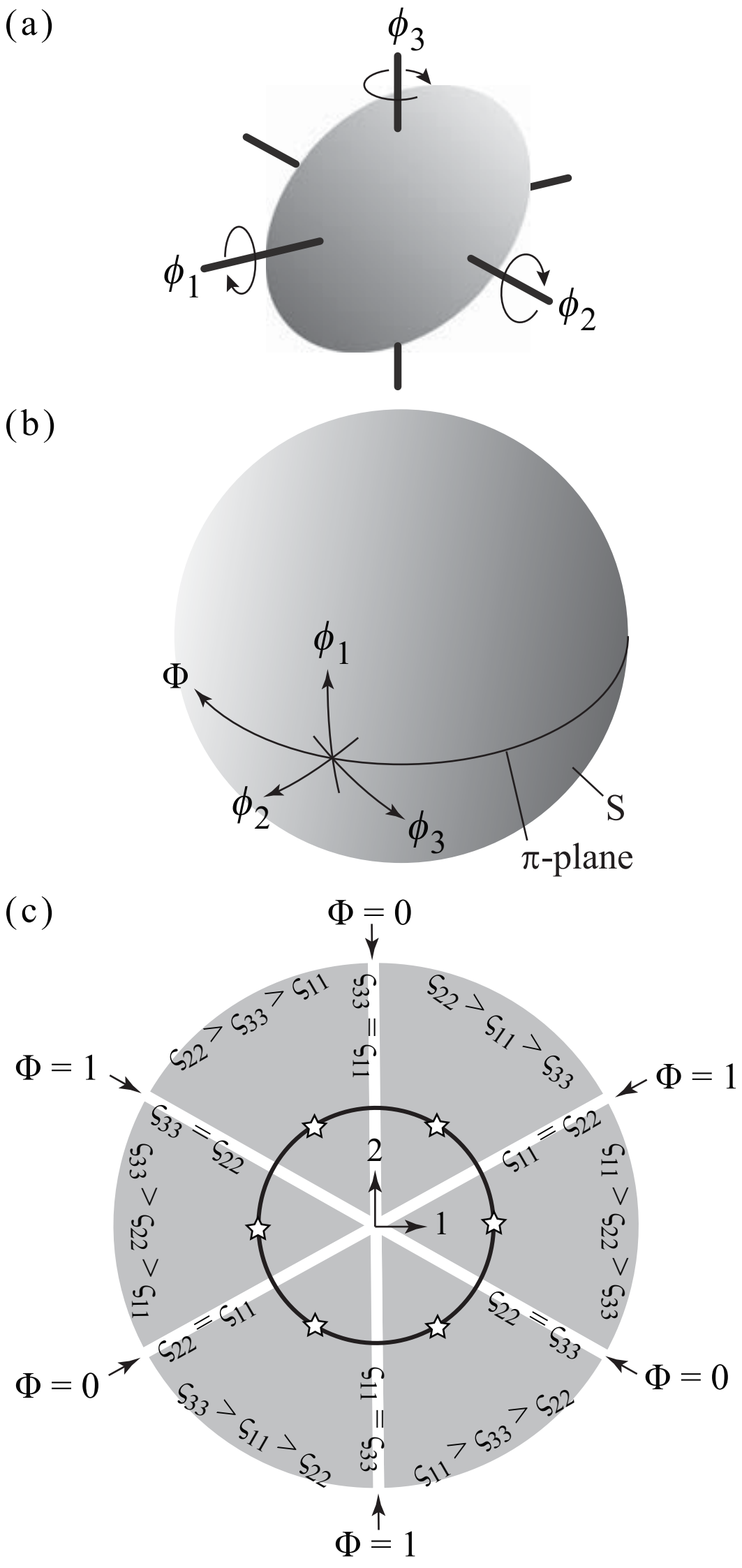
(a)
ϕ_3
ϕ_1
ϕ_2
(b)
ϕ_1
Φ
ϕ_2
ϕ_3
S
π-plane
(c)
Φ = 0
Φ = 1
Φ = 1
Φ = 0
Φ = 0
Φ = 1
$\varsigma_{33} = \varsigma_{11}$
$\varsigma_{22} > \varsigma_{11} > \varsigma_{33}$
$\varsigma_{22} > \varsigma_{33} > \varsigma_{11}$
$\varsigma_{11} = \varsigma_{22}$
$\varsigma_{33} = \varsigma_{22}$
$\varsigma_{11} > \varsigma_{22} > \varsigma_{33}$
$\varsigma_{33} > \varsigma_{22} > \varsigma_{11}$
$\varsigma_{22} = \varsigma_{33}$
$\varsigma_{22} = \varsigma_{11}$
$\varsigma_{11} > \varsigma_{33} > \varsigma_{22}$
$\varsigma_{33} > \varsigma_{11} > \varsigma_{22}$
$\varsigma_{11} = \varsigma_{33}$
2
1

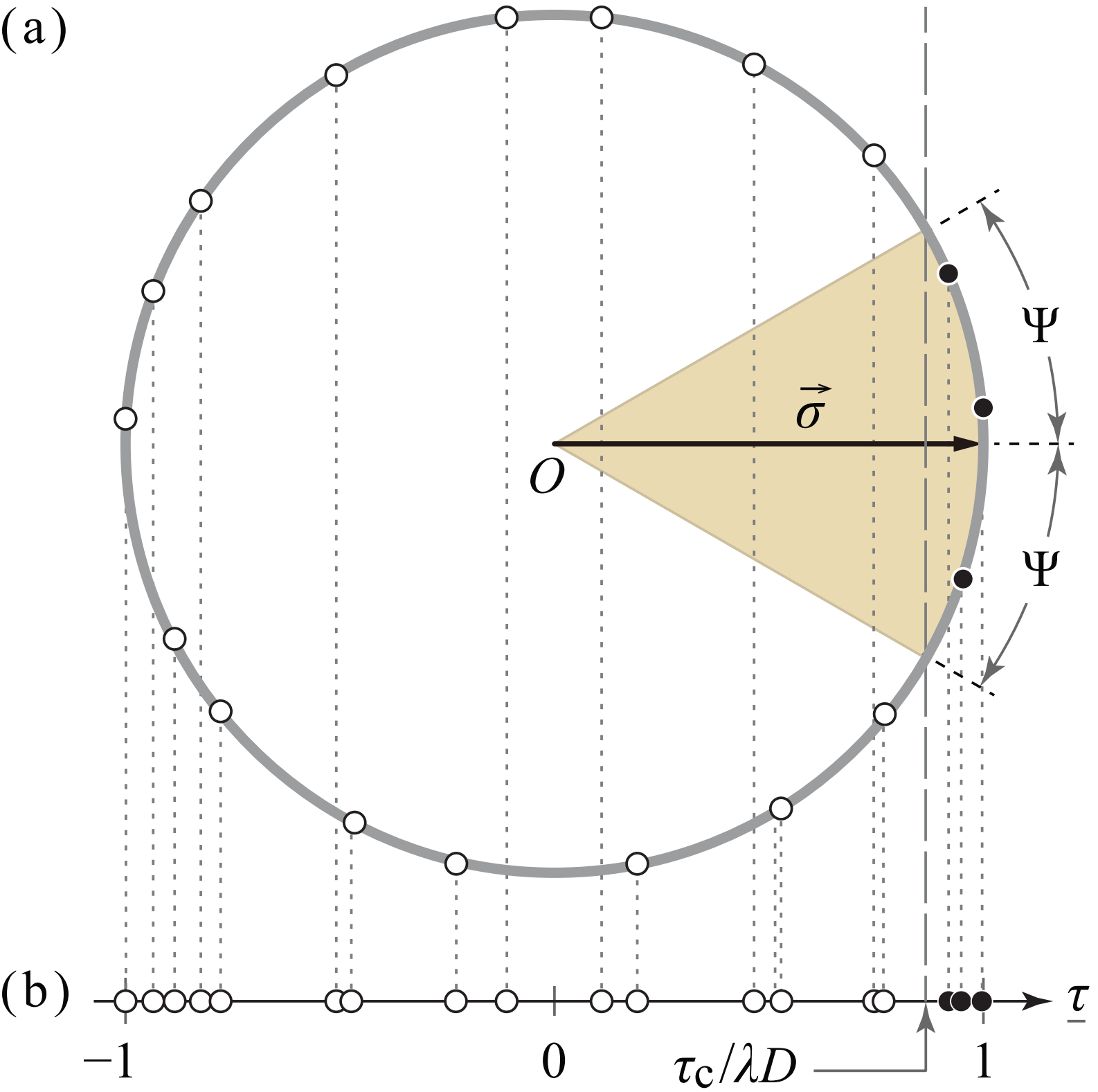
(a)
Ψ
$\vec{\sigma}$
O
Ψ
(b)
τ
−1
0
$\tau_c/\lambda D$
1

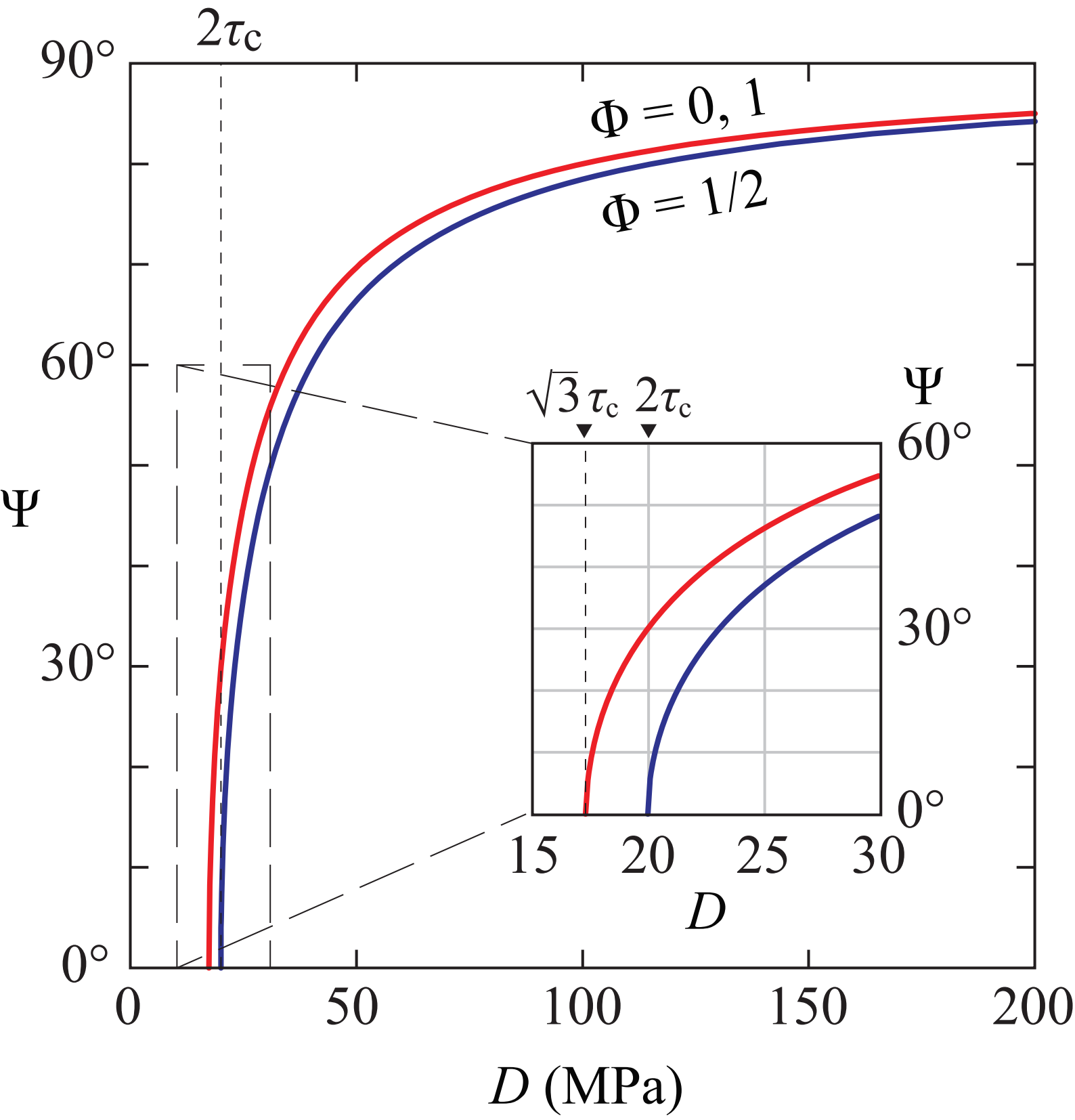
90°
60°
30°
0°
Ψ
2τc
Φ = 0, 1
Φ = 1/2
√3 τc
2τc
Ψ
60°
30°
0°
15
20
25
30
D
0
50
100
150
200
D (MPa)

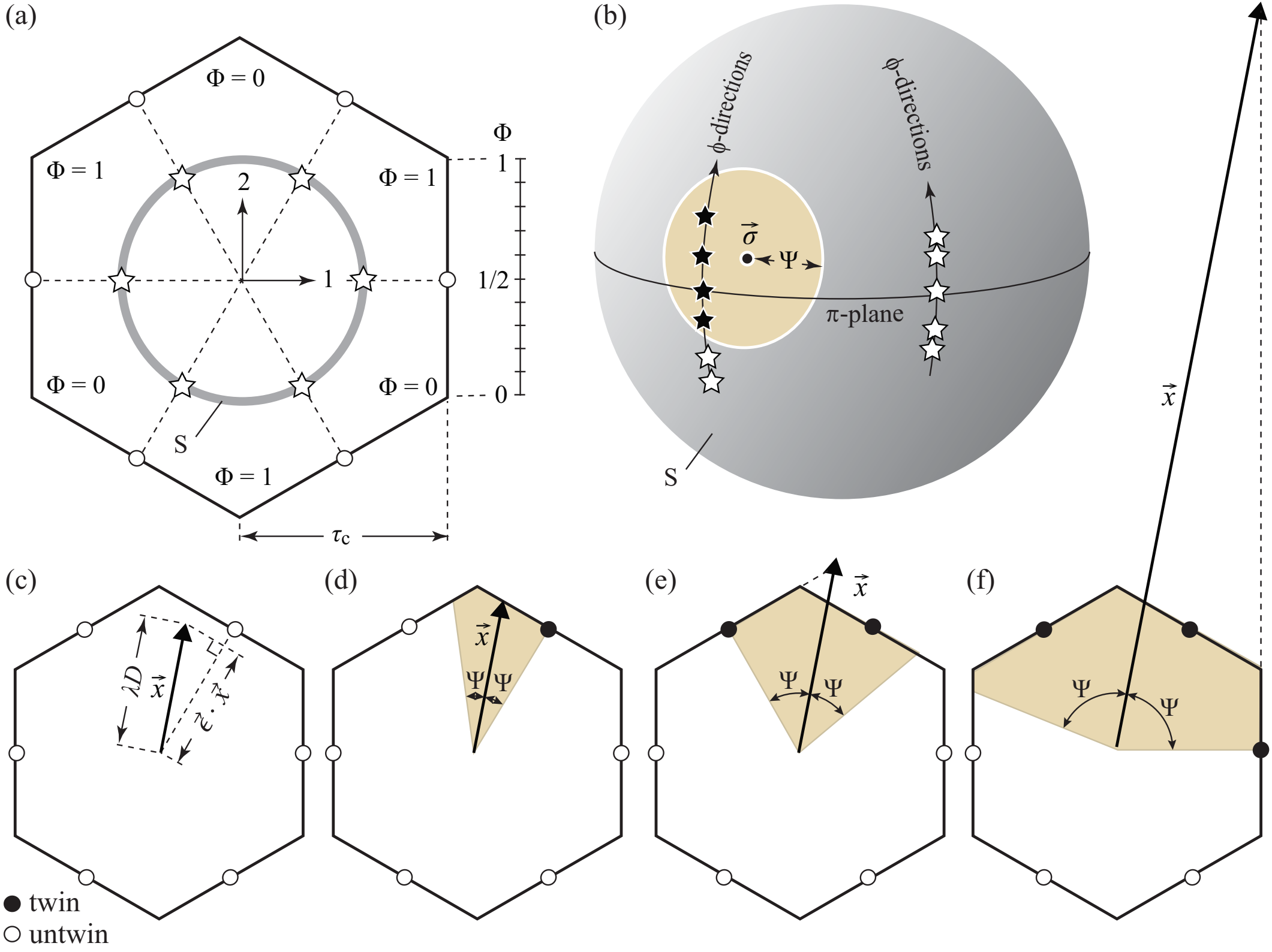
(a)
Φ = 0
Φ = 1
Φ = 1
Φ = 0
Φ = 0
Φ = 1
2
1
Φ
1
1/2
0
S
τ_c
(b)
ϕ-directions
ϕ-directions
$\vec{\sigma}$
Ψ
π-plane
S
$\vec{x}$
(c)
λD
$\vec{x}$
$\vec{\epsilon}\cdot\vec{x}$
(d)
$\vec{x}$
Ψ
Ψ
(e)
$\vec{x}$
Ψ
Ψ
(f)
Ψ
Ψ
twin
untwin

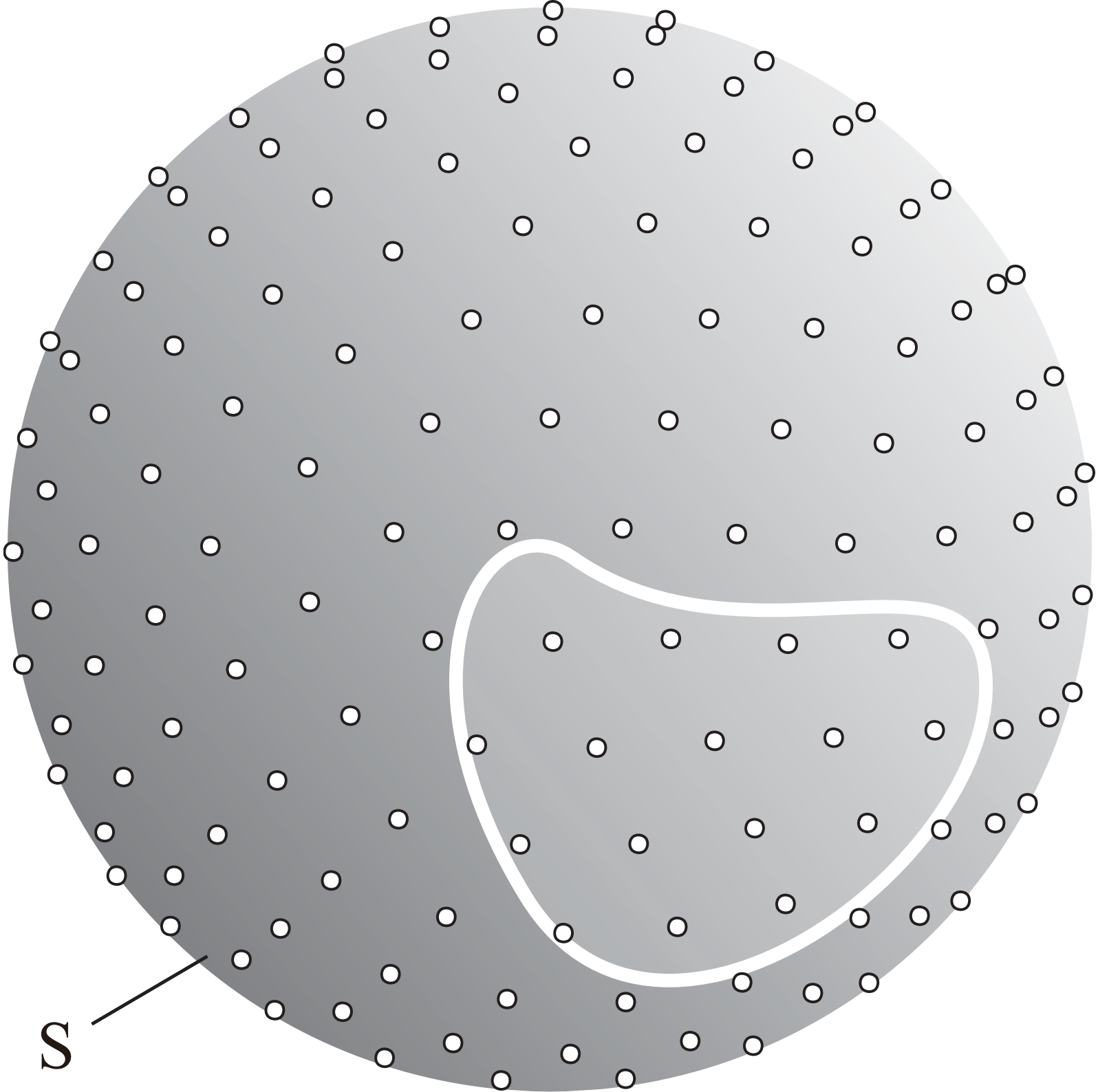
S

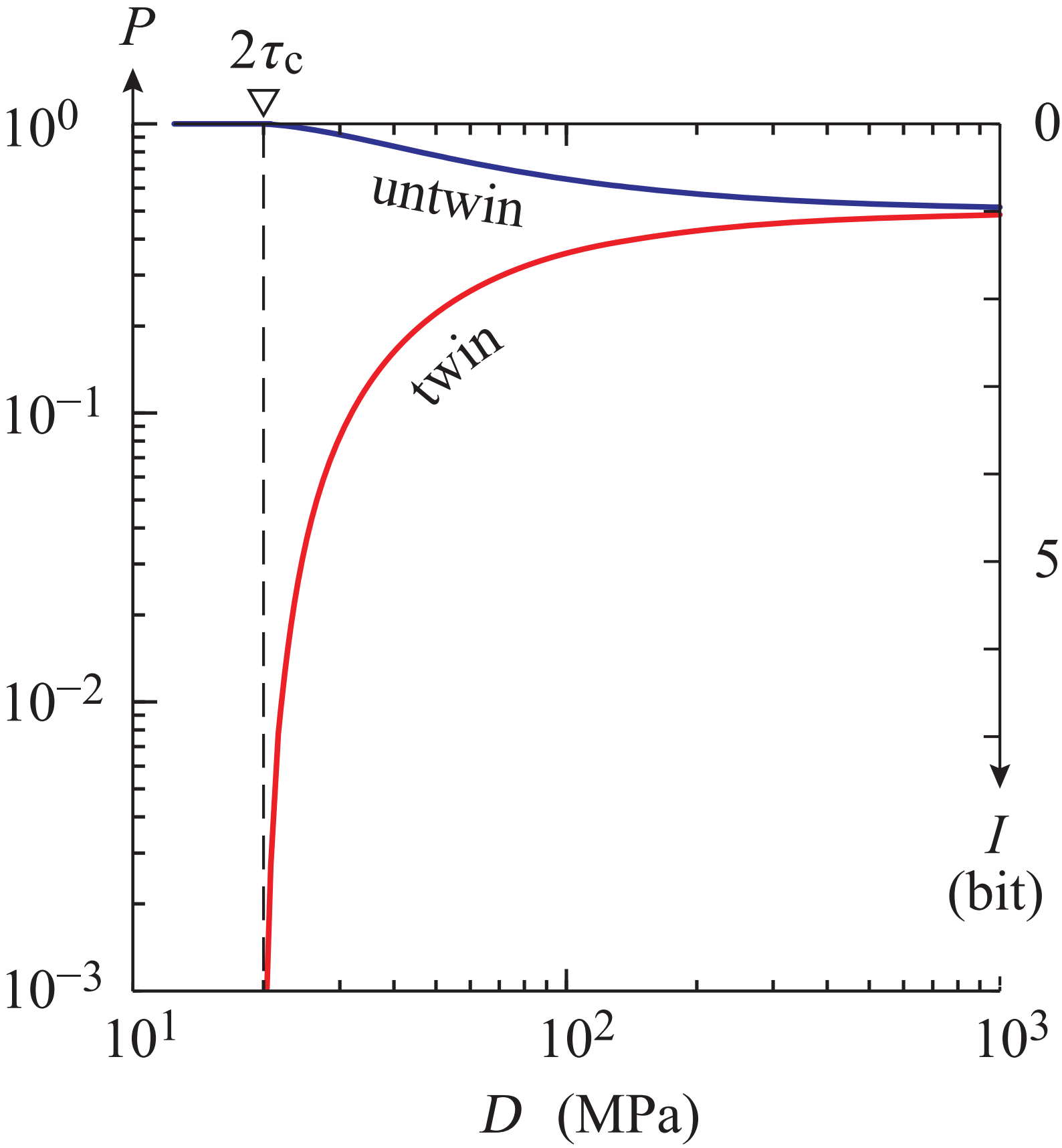
P
2τc
10^0
10^−1
10^−2
10^−3
untwin
twin
0
5
I
(bit)
10^1
10^2
10^3
D (MPa)

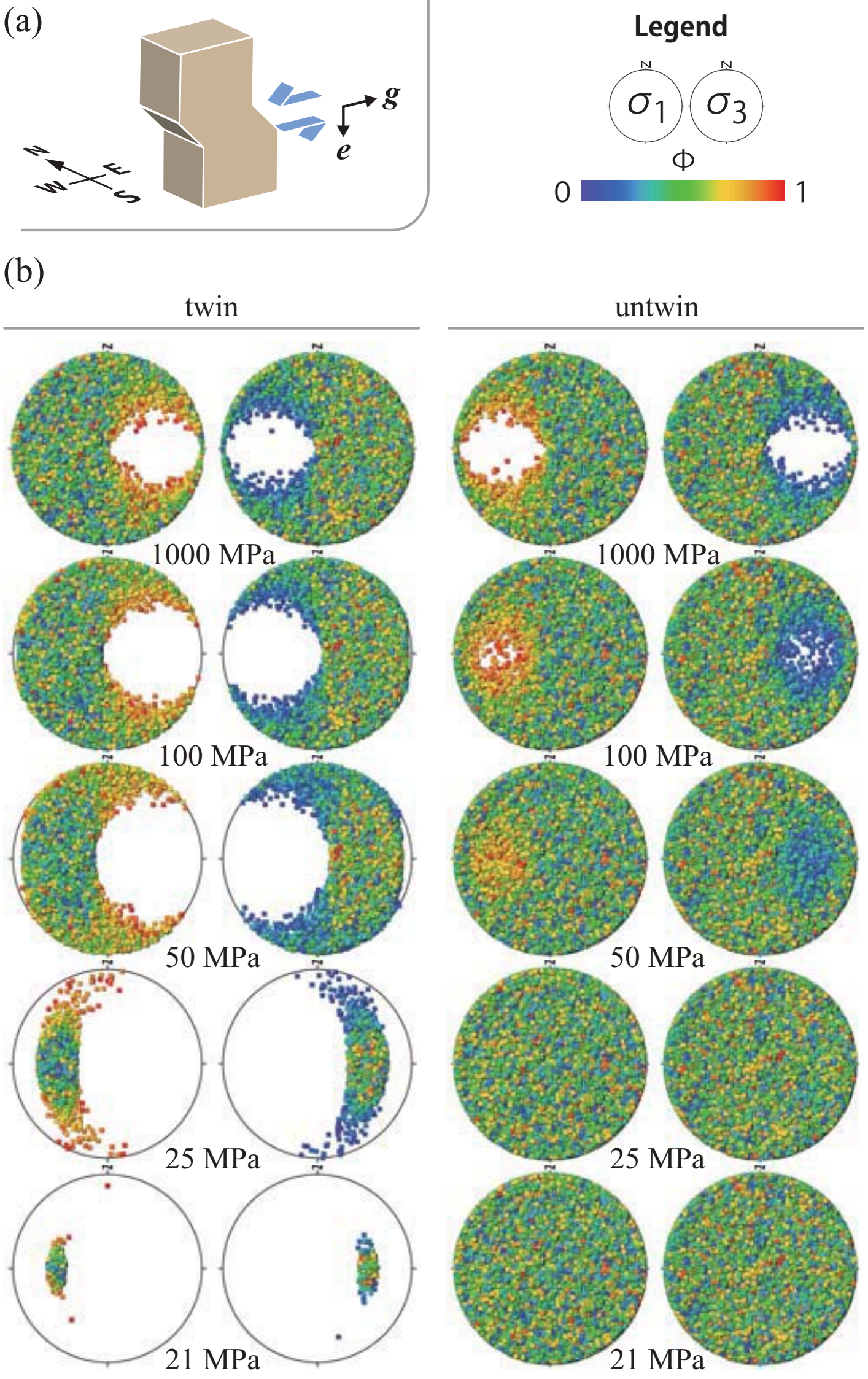
(a)
g
e
N
E
W
S
Legend
N
N
σ1
σ3
Φ
0
1
(b)
twin
untwin
1000 MPa
1000 MPa
100 MPa
100 MPa
50 MPa
50 MPa
25 MPa
25 MPa
21 MPa
21 MPa

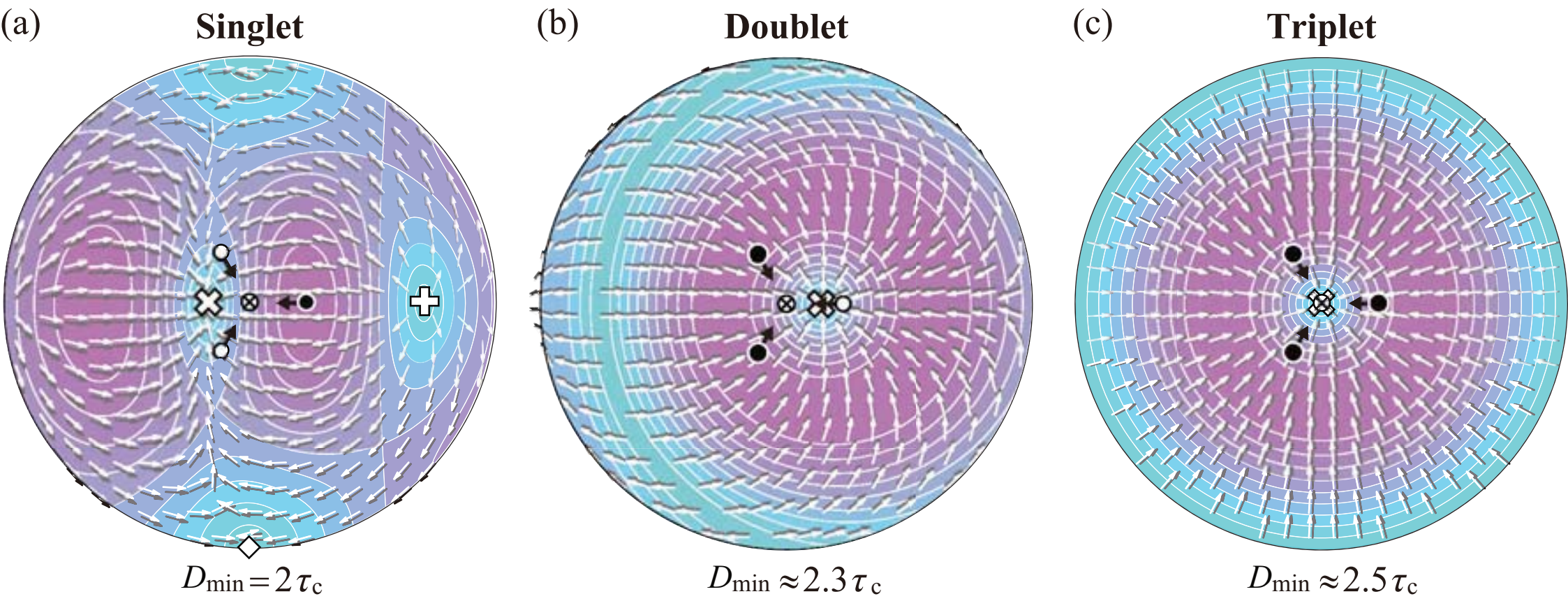
(a)
Singlet
(b)
Doublet
(c)
Triplet
$D_{\min} = 2\tau_c$
$D_{\min} \approx 2.3\tau_c$
$D_{\min} \approx 2.5\tau_c$
Legend
c
e (twin)
e (untwin)
σ1-axis
σ2-axis
σ3-axis
|τ|
0
D/2

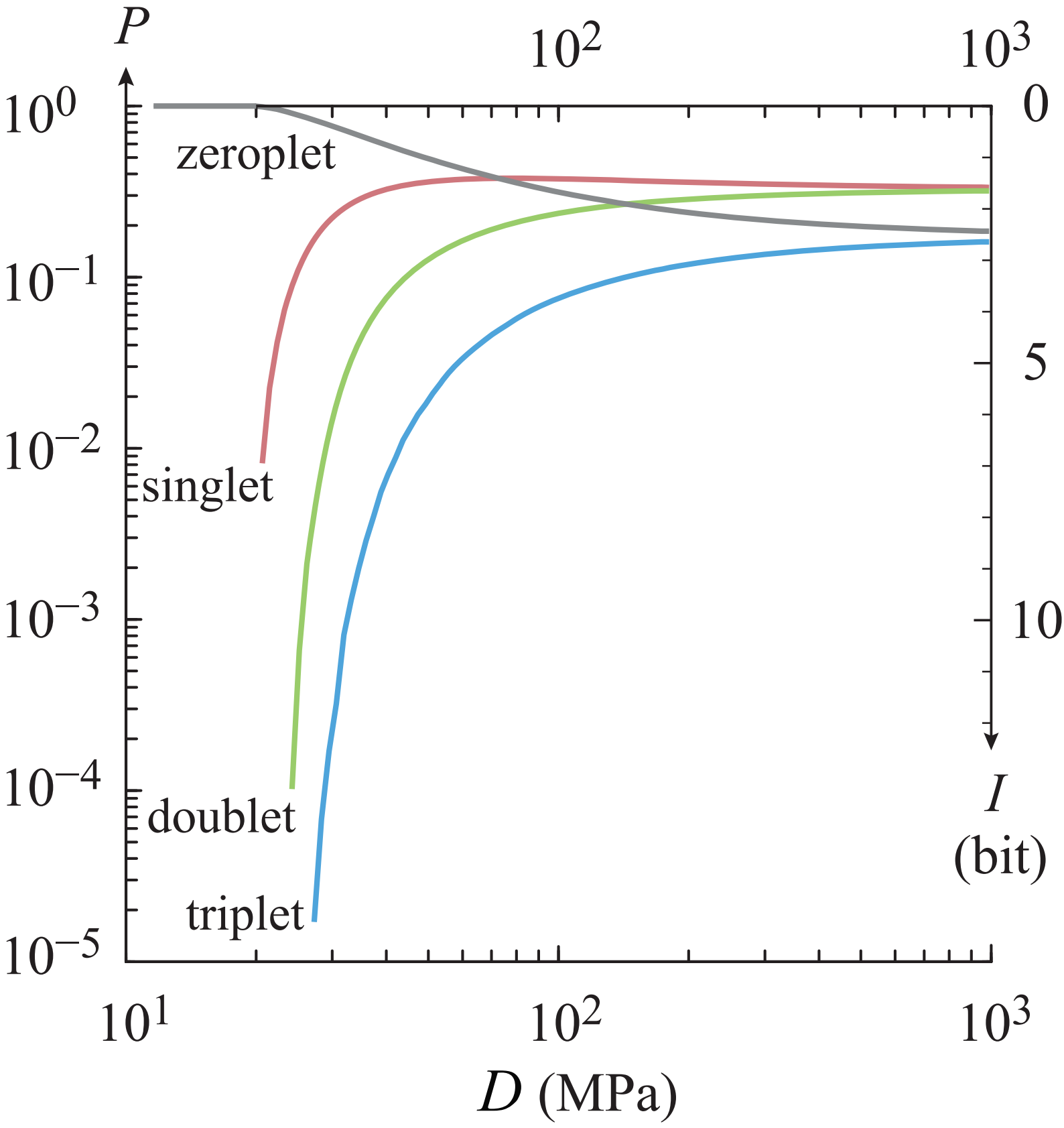
P
10^2
10^3
10^0
0
zeroplet
10^−1
5
10^−2
singlet
10^−3
10
10^−4
I
(bit)
doublet
triplet
10^−5
10^1
10^2
10^3
D (MPa)

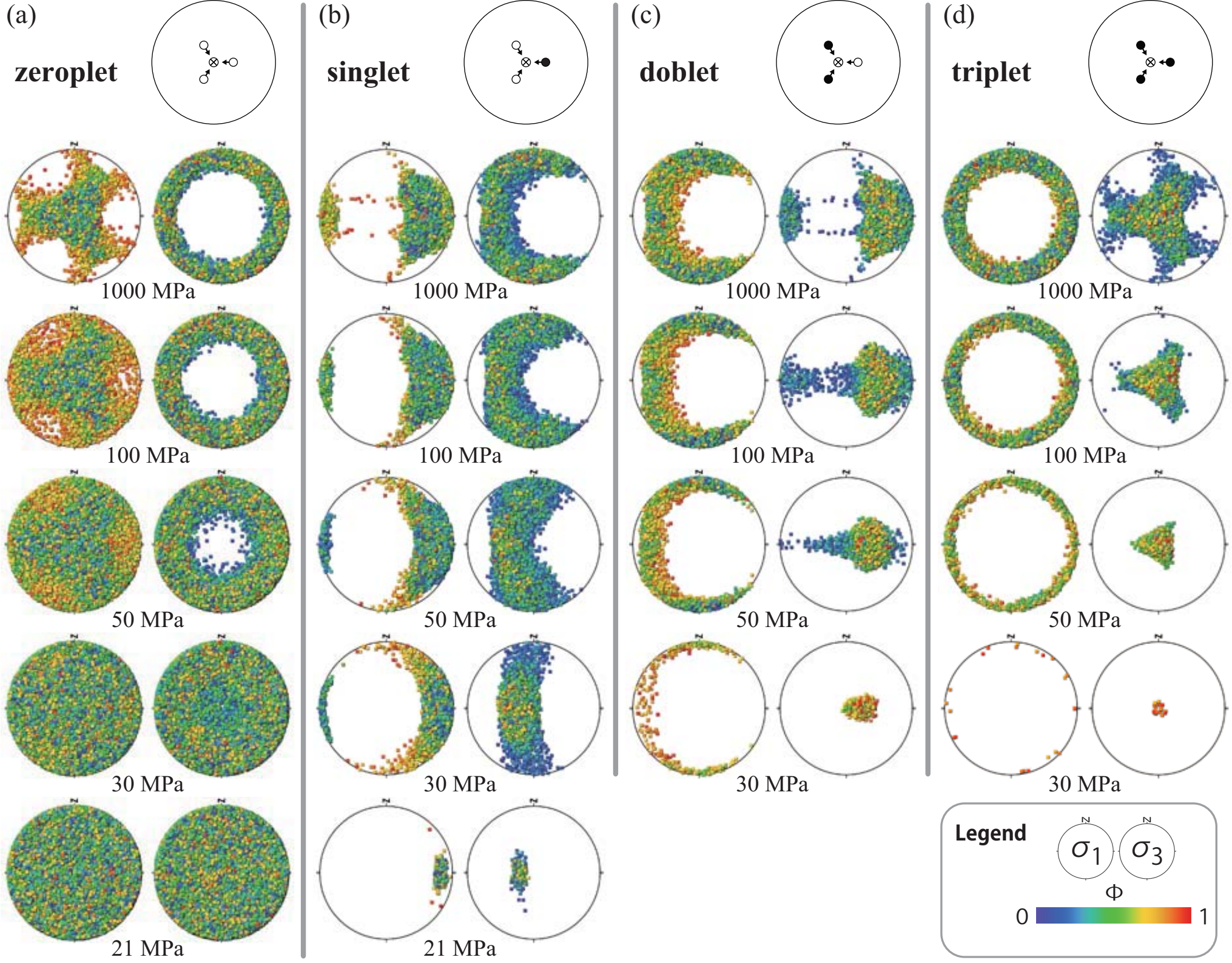
(a)
zeroplet
(b)
singlet
(c)
doblet
(d)
triplet
1000 MPa
100 MPa
50 MPa
30 MPa
21 MPa
Legend
σ1
σ3
Φ
0
1

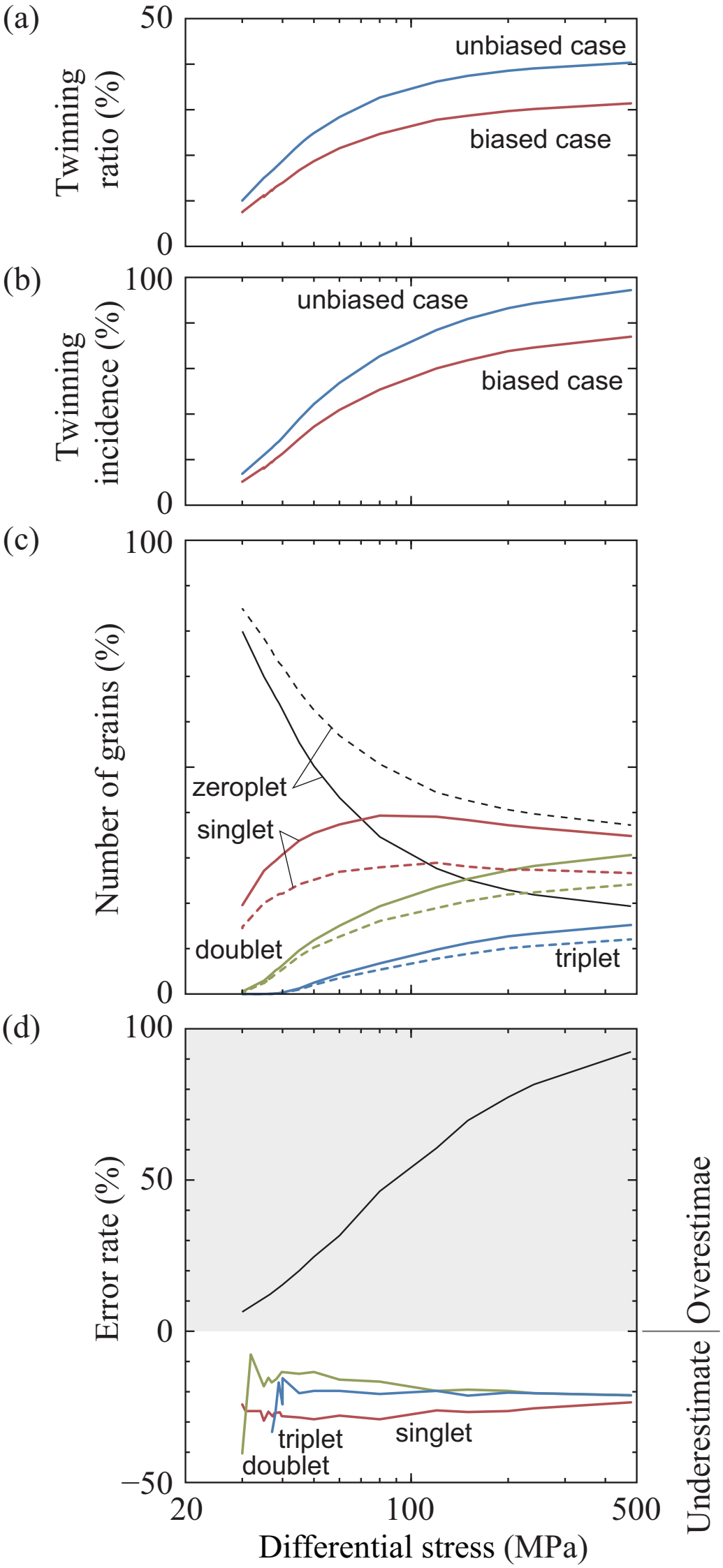
(a)
50
0
Twinning ratio (%)
unbiased case
biased case
(b)
100
0
Twinning incidence (%)
unbiased case
biased case
(c)
100
0
Number of grains (%)
zeroplet
singlet
doublet
triplet
(d)
100
50
0
−50
Error rate (%)
triplet
doublet
singlet
Overestimae
Underestimate
20
100
500
Differential stress (MPa)